

Last Revision June 9, 2022

**ICE, CLOUD, and Land Elevation Satellite-2
(ICESat-2) Project**

**Algorithm Theoretical Basis Document (ATBD)
For
Land-Ice Along-Track Products Part 2:
Slope-Corrected Land Ice Height Time Series**

**Prepared By: Benjamin Smith, Suzanne Dickinson
Kaitlin Harbeck, Tom Neumann, David Hancock, Jeffery Lee, Benjamin Jelly**



**National Aeronautics and
Space Administration**

**Goddard Space Flight Center
Greenbelt, Maryland**

CHECK <https://icesatiimis.gsfc.nasa.gov>

TO VERIFY THAT THIS IS THE CORRECT VERSION PRIOR TO USE.

29

Abstract

30

31

CM Foreword

32 This document is an Ice, Cloud, and Land Elevation Satellite-2 (ICESat-2) Project Science
33 Office controlled document. Changes to this document require prior approval of the Science
34 Development Team ATBD Lead or designee. Proposed changes shall be submitted in the
35 ICESat-II Management Information System (MIS) via a Signature Controlled Request (SCoRe),
36 along with supportive material justifying the proposed change.

37 In this document, a requirement is identified by “shall,” a good practice by “should,” permission
38 by “may” or “can,” expectation by “will,” and descriptive material by “is.”

39 Questions or comments concerning this document should be addressed to:

40 ICESat-2 Project Science Office

41 Mail Stop 615

42 Goddard Space Flight Center

43 Greenbelt, Maryland 20771

44

45
46
47
48
49
50
51
52
53
54
55
56
57
58
59
60
61
62
63
64
65
66
67

Preface

This document is the Algorithm Theoretical Basis Document for the TBD processing to be implemented at the ICESat-2 Science Investigator-led Processing System (SIPS). The SIPS supports the ATLAS (Advance Topographic Laser Altimeter System) instrument on the ICESat-2 Spacecraft and encompasses the ATLAS Science Algorithm Software (ASAS) and the Scheduling and Data Management System (SDMS). The science algorithm software will produce Level 0 through Level 4 standard data products as well as the associated product quality assessments and metadata information.

The ICESat-2 Science Development Team, in support of the ICESat-2 Project Science Office (PSO), assumes responsibility for this document and updates it, as required, as algorithms are refined or to meet the needs of the ICESat-2 SIPS. Reviews of this document are performed when appropriate and as needed updates to this document are made. Changes to this document will be made by complete revision.

Changes to this document require prior approval of the Change Authority listed on the signature page. Proposed changes shall be submitted to the ICESat-2 PSO, along with supportive material justifying the proposed change.

Questions or comments concerning this document should be addressed to:

Thorsten Markus, ICESat-2 Project Scientist
Mail Stop 615
Goddard Space Flight Center
Greenbelt, Maryland 20771

68

Review/Approval Page

Prepared by:

Benjamin Smith
Principal Researcher
University of Washington
Applied Physics Lab Polar Science Center
1013 NE 40th Street
Box 355640
Seattle, WA 98105

Reviewed by:

*Shane Grigsby
Postdoctoral Scholar
Colorado School of Mines
Department of Geophysics*

*Ellen Enderlin
Assistant Professor
Department of Geosciences
Boise State University*

Approved by:

*Tom Neumann
Project Scientist
Code 615*

69

70

71

*** Signatures are available on-line at: <https://icesatiimis.gsfc.nasa.gov> ***

Change History Log

Revision Level	Description of Change	SCoRe No.	Date Approved
1.0	Initial Release		
1.1	Changes for release 002. Calculate all crossovers (including near 88 S), determine the center of the y_atc search from the median of unique pair center locations.		
1.2	Changes for release 003. Add geoid and dem parameters.		
1.3	Improved the description of the polynomial coefficient writing process		
1.4	Changes for release 005: Updated geoid description, changed product name		

73

List of TBDs/TBRs

Item No.	Location	Summary	Ind./Org.	Due Date

74

75	Table of Contents	
76	Abstract	ii
77	CM Foreword.....	iii
78	Preface.....	iv
79	Review/Approval Page.....	v
80	Change History Log.....	vi
81	List of TBDs/TBRs.....	vii
82	Table of Contents.....	viii
83	List of Figures	x
84	List of Tables	xi
85	1.0 INTRODUCTION	1
86	2.0 BACKGROUND INFORMATION and OVERVIEW.....	2
87	2.1 Background.....	2
88	2.2 Elevation-correction Coordinate Systems.....	3
89	2.3 Terminology:	3
90	2.4 Repeat and non-repeat cycles in the ICESat-2 mission	5
91	2.5 Physical Basis of Measurements / Summary of Processing.....	5
92	2.5.1 Choices of product dimensions	6
93	2.6 Product coverage.....	6
94	3.0 ALGORITHM THEORY: Derivation of Land Ice H (t)/ATL11 (L3B).....	8
95	3.1 Input data editing	10
96	3.1.1 Input data editing using ATL06 parameters.....	12
97	3.1.2 Input data editing by slope.....	13
98	3.1.3 Spatial data editing	14
99	3.2 Reference-Surface Shape Correction.....	14
100	3.2.1 Reference-surface shape inversion	15
101	3.2.2 Misfit analysis and iterative editing	16
102	3.3 Reference-shape Correction Error Estimates.....	17
103	3.4 Calculating corrected height values for repeats with no selected pairs	17
104	3.5 Calculating systematic error estimates	17
105	3.6 Calculating shape-corrected heights for crossing-track data.....	18

106	3.7	Calculating parameter averages	19
107	3.8	Output data editing	19
108	4.0	LAND ICE PRODUCTS: Land Ice H (t)(ATL 11/L3B)	20
109	4.1	File naming convention	21
110	4.2	/ptx group	21
111	4.3	/ptx/ref_surf group	22
112	4.4	/ptx/cycle_stats group	25
113	4.5	/ptx/crossing_track_data group	26
114	5.0	ALGORITHM IMPLEMENTATION	29
115	5.1.1	Select ATL06 data for the current reference point.....	30
116	5.1.2	Select pairs for the reference-surface calculation	30
117	5.1.3	Adjust the reference-point y location to include the maximum number of	
118		cycles 32	
119	5.1.4	Calculate the reference surface and corrected heights for selected pairs	33
120	5.1.5	Calculate corrected heights for cycles with no selected pairs.	36
121	5.1.6	Calculate corrected heights for crossover data points.....	37
122	5.1.7	Provide error-averaged values for selected ATL06 parameters	38
123	5.1.8	Provide miscellaneous ATL06 parameters	39
124	5.1.9	Characterize the reference surface	40
125	6.0	Appendix A: Glossary	42
126	7.0	Browse products.....	48
127		Glossary/Acronyms.....	54
128		References	55
129			

130 **List of Figures**

131

132	<u>Figure</u>	<u>Page</u>
133	Figure 2-1. ICESat-2 repeat-track schematic.....	3
134	Figure 2-2. ATL06 data for an ATL11 reference point.....	4
135	Figure 2-3. Potential ATL11 coverage	6
136	Figure 3-1. ATL11 fitting schematic	9
137	Figure 3-2. Data selection.....	12
138	Figure 5-1 Flow Chart for ATL11 Surface-shape Corrections.....	29
139	Figure 6-1. Spots and tracks, forward flight	45
140	Figure 6-2. Spots and tracks, backward flight	46
141	Figure 6-3. Granule regions	47
142		

143
144
145
146
147
148
149
150
151

List of Tables

<u>Table</u>	<u>Page</u>
Table 3-1 Parameter Filters to determine the validity of segments for ATL11 estimates	11
Table 4-1 Parameters in the <i>/ptx/</i> group	22
Table 4-2 Parameters in the <i>/ptx/ref_surf</i> group	23
Table 4-3 Parameters in the <i>/ptx/cycle_stats</i> group	25
Table 4-4 Parameters in the <i>/ptx/crossing_track_data</i> group	27

152 **1.0 INTRODUCTION**

153 This document describes the theoretical basis and implementation of the level-3b land-ice
154 processing algorithm for ATL11, which provides time series of surface heights. The higher-level
155 products, providing gridded height, and gridded height change will be described in supplements
156 to this document available in early 2020.

157 ATL11 is based on the ICESat-2 ATL06 Land-ice Height product, which is described elsewhere
158 (Smith and others, 2019a, Smith and others, 2019b). ATL06 provides height estimates for 40-
159 meter overlapping surface segments, whose centers are spaced 20 meters along each of ICESat-
160 2's RPTs (reference pair tracks) but displaced horizontally both relative to the RPT and relative
161 to one another because of small (a few tens of meters or less) imprecisions in the satellite's
162 control of the measurement locations on the ground. ATL11 provides heights corrected for these
163 offsets between the reference tracks and the location of the ATLAS measurements. It is intended
164 as an input for high-level products, ATL15 and ATL16, which will provide gridded estimates of
165 ice-sheet height and height change, but also may be used alone, as a spatially-organized product
166 that allows easy access to height-change information derived from ICESat-2.

167 ATL11 employs a technique which builds upon those previously used to measured short-term
168 elevation changes using ICESat repeat-track data. Where surface slopes are small and the
169 geophysical signals are large compared to background processes (i.e., ice plains and ice shelves),
170 some studies have subtracted the mean from a collection of height measurements from the same
171 repeat track to leave the rapidly-changing components associated with subglacial water motion
172 (Fricker and others, 2007) or tidal flexure (Brunt and others, 2011). In regions where off-track
173 surface slopes are not negligible, height changes can be recovered if the mean height and an
174 estimate of the surface slope (Smith and others, 2009) are subtracted from the data, although in
175 these regions the degree to which the surface slope estimate and the elevation-change pattern are
176 independent is challenging to quantify.

177 ICESat-2's ATL06 product provides both surface height and surface-slope information each time
178 it overflies its reference tracks. The resulting data are similar to that from the scanning laser
179 altimeters that have been deployed on aircraft in Greenland and Antarctica for two decades
180 (cite), making algorithms originally developed for these instruments appropriate for use in
181 interpreting ATLAS data. One example is the SERAC (Surface Elevation Reconstruction and
182 Change Detection) algorithm (Schenk & Csatho, 2012) provides an integrated framework for the
183 derivation of elevation change from altimetry data. In SERAC, polynomial surfaces are fit to
184 collections of altimetry data in small (< 1 km) patches, and these surfaces are used to correct the
185 data for sub-kilometer surface topography. The residuals to the surface then give the pattern of
186 elevation change, and polynomial fits to the residuals as a function of time give the long-term
187 pattern of elevation change. The ATL11 algorithm is similar to SERAC, except that (1)
188 polynomial fit correction is formulated somewhat differently, so that the ATL11 correction gives
189 the surface height at the fit center, not the height residual, and (2) ATL11 does not include a
190 polynomial fit with respect to time.
191

192 2.0 BACKGROUND INFORMATION AND OVERVIEW

193 This section provides a conceptual description of ICESat-2's ice-sheet height measurements and
194 gives a brief description of the derived products.

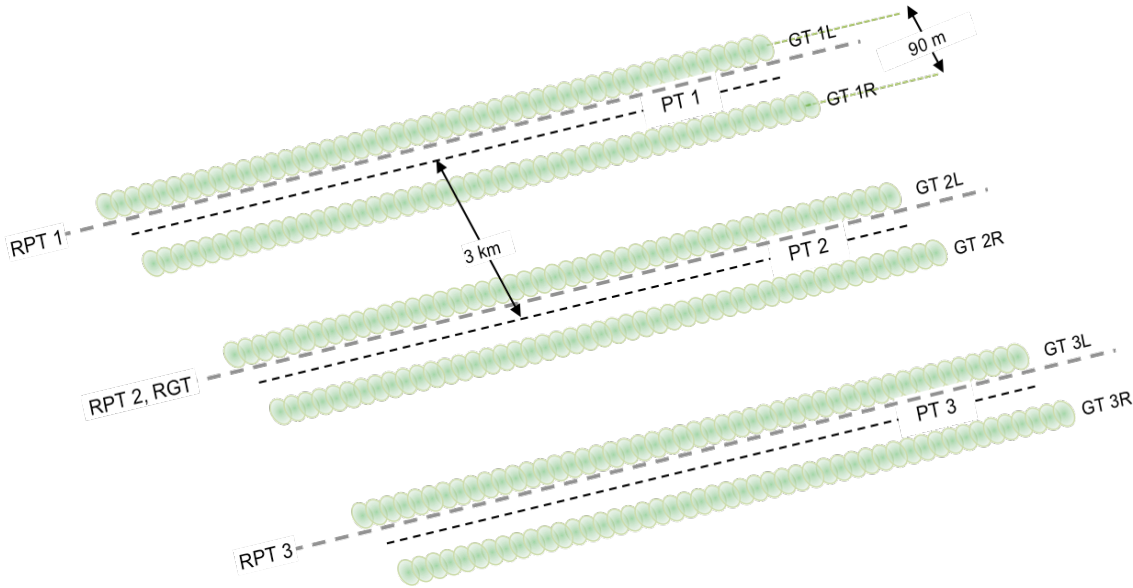
195 2.1 Background

196 The primary goal of the ICESat-2 mission is to estimate mass-balance rates for the Earth's ice
197 sheets. An important step in this process is the calculation of height change at specific locations
198 on the ice sheets. In an ideal world, a satellite altimeter would exactly measure the same point
199 on the earth on each cycle of its orbit. However, there are limitations in a spacecraft's ability to
200 exactly repeat the same orbit and to point to the same location. These capabilities are greatly
201 improving with technological advances but still have limits that need to be accounted for when
202 estimating precise elevation changes from satellite altimetry data. The first ICESat mission
203 allowed estimates of longer-term elevation rates using along-track differencing, because
204 ICESat's relatively precise (50-150-m) pointing accuracy, precise (4-15 m) geolocation
205 accuracy, and small (35-70-m) footprints allowed it to resolve small-scale ice-sheet topography.
206 However, because ICESat had a single-beam instrument, its repeat-track measurements were
207 reliable only for measuring the mean rate of elevation change, because shorter-term height
208 differences could be influenced by the horizontal dispersion of tracks on a sloping surface.
209 ICESat-2 makes repeat measurements over a set of 1387 reference ground tracks (RGTs),
210 completing a *cycle* over all of these tracks every 91 days. ICESat-2's ATLAS instrument
211 employs a split-beam design, where each laser pulse is divided six separate beams. The beams
212 are organized into three *beam pairs*, with each separated from its neighbors by 3.3 km (**Figure**
213 **2-1**), each pair following a reference pair track (RPT) that is parallel to the RGT. The beams
214 within each pair separated by 90 m, which means that each cycle's measurement over an RPT
215 can determine the surface slope independently, and a height difference can be derived from
216 any two measurements of an RPT. The 90-m spacing between the laser beams in each pair
217 is equal to twice the required RMS accuracy with which ICESat-2 can be pointed at its RPTs,
218 which means that for most, but not all, repeat measurements of a given RPT, the pairs of
219 beams will overlap one another. To obtain a record of elevation change from the collection
220 of paired measurements on each RPT, some correction is still necessary to account for the
221 effects of small-scale surface topography around the RPT in the ATL06 surface heights that
222 appear as a result of this non-exact pointing. ATL11 uses a polynomial fit to the ATL06
223 measurements to correct for small-scale topography effects on surface heights that result
224 from this non-exact pointing.

225 The accuracy of ICESat-2 measurements depends on the thickness of clouds between the
226 satellite and the surface, on the reflectance, slope, and roughness of the surface, and on
227 background noise rate which, in turn, depends on the intensity of solar illumination of the
228 surface and the surface reflectance. It also varies from laser beam to beam, because in each
229 of ICESat-2's beam pairs one beam (the "strong beam") has approximately four times the
230 signal strength of the other (the "weak beam"). Parameters on the ATL06 product allow
231 estimation of errors in each measurement, and allow filtering of most measurements with
232 large errors due to misidentification of clouds or noise as surface returns (blunders), but to

233 enable higher precision surface change estimates, ATL11 implements further self-
 234 consistency checks that further reduce the effects of errors and blunders.
 235

Figure 2-1. ICESat-2 repeat-track schematic



Schematic drawing showing the pattern made by ATLAS's 6-beam configuration on the ground, for a track running from lower left to upper right. The 6 beams are grouped into 3 beam pairs with a separation between beams within a pair of 90m and a separation between beam pairs of 3.3 km. The RPTs (Reference Pair Tracks, heavily dashed lines in gray) are defined in advance of launch; the central RPT follows the RGT (Reference Ground Track, matching the nadir track of the predicted orbit). The Ground Tracks are the tracks actually measured by ATLAS (GT1L, GT1R, etc., shown by green footprints). Measured Pair Tracks (PTs, smaller dashed lines in black) are defined by the centers of the pairs of GTs, and deviate slightly from the RPTs because of inaccuracies in repeat-track pointing. The separation of GTs in each pair in this figure is greatly exaggerated relative to the separation of the PTs.

236 **2.2 Elevation-correction Coordinate Systems**

237 We perform ATL11 calculations using the along-track coordinate system described in the
 238 ATL06 ATBD (Smith and others, 2019b, Smith and others, 2019a). The along-track coordinate
 239 is measured parallel to the RGT, starting at each RGT's origin at the equator. The across-track
 240 coordinate is measured to the left of the RGT, so that the two horizontal basis vectors and the
 241 local vertical vector form a right-handed coordinate system.

242 **2.3 Terminology:**

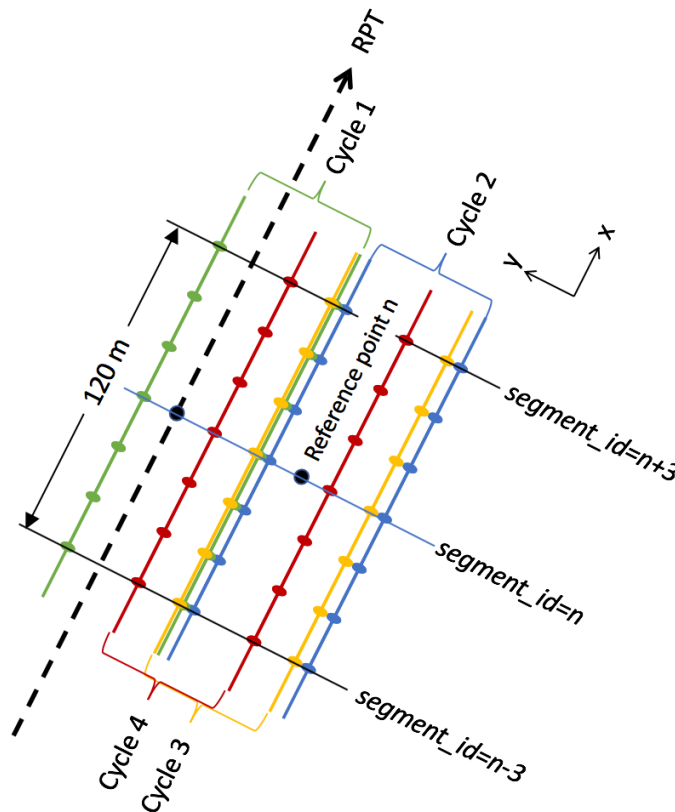
243 Some of the terms that we will use in describing the ATL11 fitting process and the data
 244 contributing are:

245 *RPT*: Reference pair track

246 *Cycle*: ICESat-2 has 1387 distinct reference ground tracks, which its orbit covers every 91 days.
 247 One repeat measurement of these reference ground tracks constitutes a cycle.
 248 *ATL06 segment*: A 40-meter segment fit to a collection of ATL03 photon-event data, as
 249 described in the ATL06 ATBD
 250 *ATL06 pair*: Two ATL06 segments from the same cycle with the same *segment_id*. By
 251 construction, both segments in the ATL06 pair have the same along-track coordinate, and are
 252 separated by the beam-to-beam spacing (approximately 90 m) in the across-track direction
 253 *ATL11 RPT point*: The expected location of each ATL11 point on the RPT, equivalent to the
 254 beginning of every third geosegment on the RPT, or the center of every third ATL06 segment.
 255 *ATL11 reference point*: an *ATL11 RPT point* shifted in the across-track direction to better match
 256 the geometry of the available ATL06 data.
 257 *ATL11 fit*: The data and parameters associated with a single ATL11 reference point. This
 258 includes corrected heights from all available cycles
 259

260 ATL11 calculates elevations and elevation differences based on collections of segments from the
 261 same beam pair but from different cycles. ATL11 is posted every 60 m, which corresponds to
 262 every third ATL06 *segment_id*, and includes ATL06 segments spanning three segments before
 263 and after the central segment, so that the ATL11 uses data that span 120 m in the along-track
 264 direction. ATL11 data are centered on *reference points*, which has the same along-track
 265 coordinate as its central ATL06 segment, but is displaced in the across-track direction to better
 266 match the locations of the ATL06 measurements from all of the cycles present (see section
 267 3.1.3).

Figure 2-2. ATL06 data for an ATL11 reference point



Schematic of ATL06 data for an ATL11 reference point centered on segment n, based on data from four cycles. The segment centers span 120 m in the along-track data, and the cycles are randomly displaced from the RPT in the across-track direction. The reference point has an along-track location that matches that of segment n, and an across-track position chosen to match the displacements of the cycles.

268

269 **2.4 Repeat and non-repeat cycles in the ICESat-2 mission**

270 In the early part of the ICESat-2 mission, an error in the configuration of the start trackers
271 prevented the instrument from pointing precisely at the RGTs. As a result, all data from cycles 1
272 and 2 were measured between one and two kilometers away from the RGTs, with offsets that
273 varied in time and as a function of latitude. The measurements from cycles 1 and 2 still give
274 high-precision measurements of surface height, but repeat-track measurements from ICESat-2
275 begin during cycle 3, in April of 2019. ATL11 files will be generated for ATL06 granules from
276 cycles 1 and 2, but these will contain only one cycle of data, plus crossovers, because the
277 measurements from these cycles (which are displaced from the RPTs by several kilometers) will
278 not be repeated. We expect the measurements from cycles 1 and 2 to be useful as a reduced-
279 resolution (compared to ATL06) mapping of the ice sheet, which may prove useful in DEM
280 generation and in comparisons with other altimetry missions. For cycles 3 and after, each
281 ATL11 granule will contain all available cycles for each RGT (i.e. from cycle 3 onwards), and
282 will contain crossovers between the repeat cycles and cycles 1 and 2.

283 Outside the polar regions, ICESat-2 is pointed to minimize gaps between repeat measurements,
284 and so does not make repeat measurements over its ground tracks. ATL11 is only calculated
285 within the repeat-pointing mask (see Figure ???), which covers areas poleward of 60°N and
286 60°S.

287

288 **2.5 Physical Basis of Measurements / Summary of Processing**

289 Surface slopes on the Antarctic and Greenland ice sheets are generally small, with magnitudes
290 less than two degrees over 99% of Antarctica's area. Smaller-scale (0.5-3 km) undulations,
291 generated by ice flow over hilly or mountainous terrain may have amplitudes of up to a few
292 degrees. Although we expect that the surface height will change over time, slopes and locations
293 of these smaller-scale undulation are likely controlled by underlying topography and should
294 remain essentially constant over periods of time comparable with the expected 3-7 duration of
295 the ICESat-2 mission. This allows us to use estimates of ice-sheet surface shape derived from
296 data spanning the full mission to correct for small (<130-m) differences in measurement
297 locations between repeat measurements of the same RPT, to produce records of height change
298 for specific locations. To account for changes in the ice-sheet surface slope associated with
299 gradients in thinning, we also solve for the rate of surface-slope change, when sufficient data are
300 available. Further, we can use the surface slope estimates in ATL06 to determine whether
301 different sets of measurements for the same fit center are self-consistent: We can assume that if
302 an ATL06 segment shows a slope significantly different from others measured near the same
303 reference point it likely is in error. The combination of parameters from ATL06 and these self-
304 consistency checks allows us to generate time series based on the highest-quality measurements

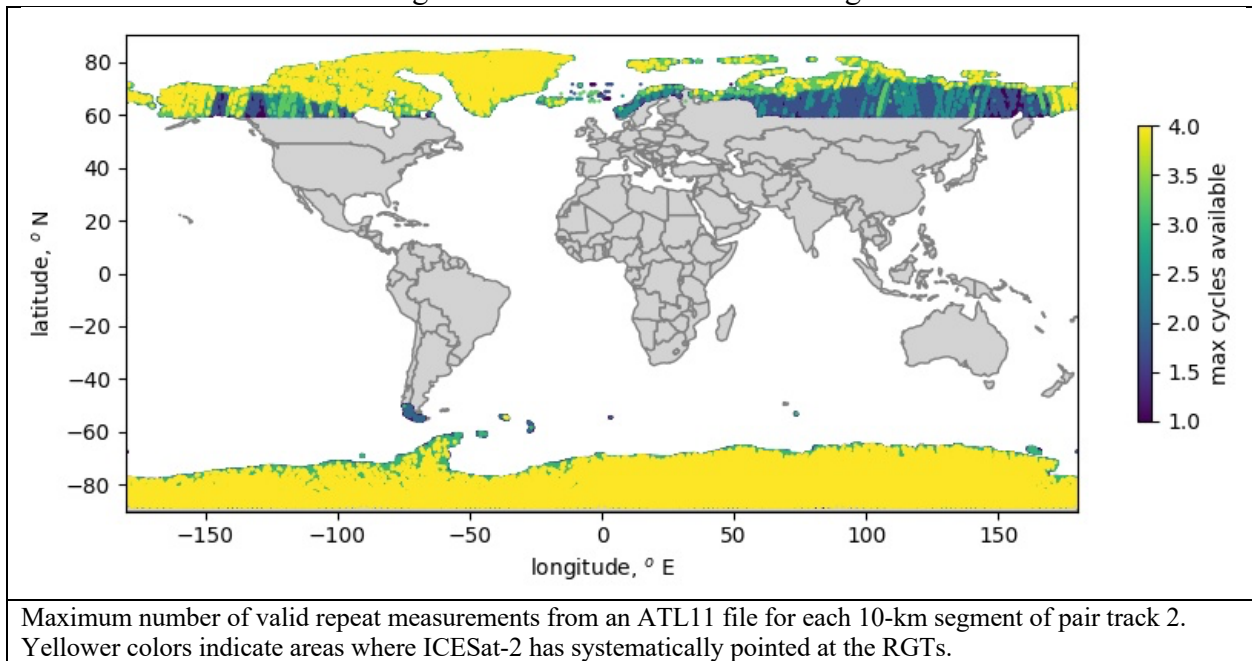
305 for each reference point, and our reference surface calculation lets us correct for small-scale
 306 topography and to estimate error magnitudes in the corrected data.

307 **2.5.1 Choices of product dimensions**

308 We have chosen a set of dimensions for the ATL11 fitting process with the goal of creating a
 309 product that is conveniently sized for analysis of elevation changes, while still capturing the
 310 details of elevation change in outlet glaciers. The assumption that ice-sheet surface can be
 311 approximated by a low-degree polynomial becomes untenable as data from larger and larger
 312 areas are included in the calculation; therefore we use data from the smallest feasible area to
 313 define our reference surface, while still including enough data to reduce the sampling error in the
 314 data and to allow for the possibility that at least one or two will encounter a flat surface, which
 315 greatly improves the chances that each cycle will be able to measure surface comparable to one
 316 another. Each ATL11 point uses data from an area up to 120 m in the along-track direction by
 317 up to 130 m in the across-track direction. We have chosen the cross-track search distance
 318 (L_{search_XT}) to be 65 m, approximately equal to half the beam spacing, plus three times the
 319 observed 6.5 m standard deviation of the across-track pointing accuracy for cycles 3 and 4 in
 320 Antarctica. We chose the across-track search distance (L_{search_AT}) to be 60 m, approximately
 321 equal to L_{search_XT} , so that the full L_{search_AT} search window spans three ATL06 segments before
 322 and after the central segment for each reference point. The resulting along-track resolution is
 323 around one third that of ATL06, but still allows 6-7 distinct elevation-change samples across a
 324 small (1-km) outlet glacier.

325 **2.6 Product coverage**

Figure 2-3. Potential ATL11 coverage



326 Over the vegetated parts of the Earth, ICESat-2 makes spatially dense measurements, measuring
 327 tracks parallel to the reference tracks in a strategy that will eventually measure global vegetation

328 with a track-to-track spacing better than 1 km. Because ATL11 relies upon repeat measurements
329 over reference tracks to allow the calculation of its reference surfaces, ATL11 is generated for
330 ICESat-2 subregions 3-5 and 10-12 (global coverage, north and south of 60 degrees). Repeat
331 measurements are limited to Antarctica, Greenland, and the High Arctic islands (Figure 2-3),
332 although in other areas the fill-in strategy developed for vegetation measurements allows some
333 repeat measurements. In regions where ICESat-2 was not pointed to the repeat track, most
334 ATL11 reference points will provide one measurement close to the RPT. Crossover data are
335 available for many of these points, though their distribution in time is not regular. A future
336 update to the product may provide crossover measurements for lower-latitude areas, but the
337 current product format is not designed to allow this.

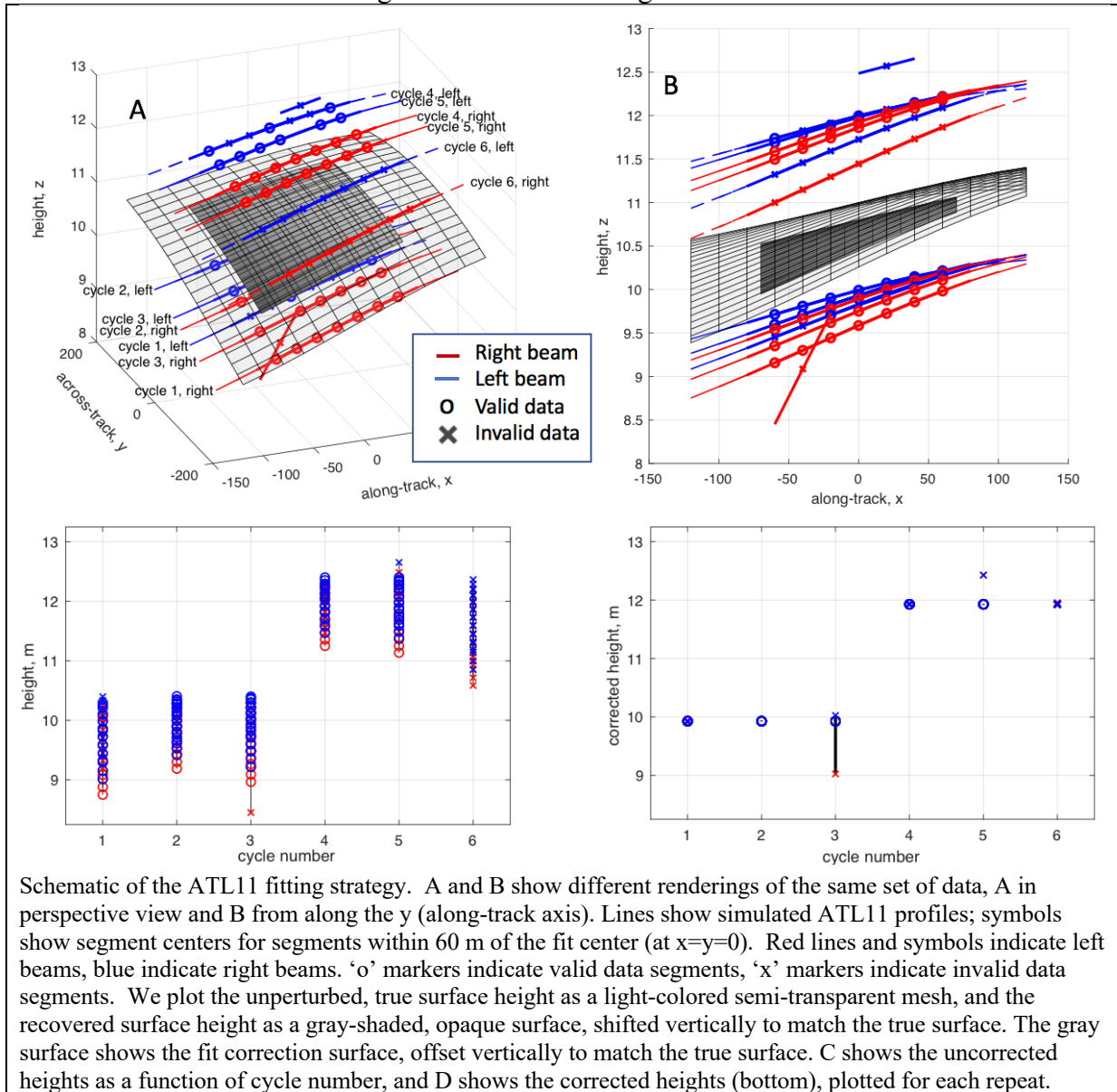
338 3.0 ALGORITHM THEORY: DERIVATION OF LAND ICE H (T)/ATL11 (L3B)

339 In this section, we describe in detail the algorithms used in calculating the ATL11 land-ice
340 parameters. This product is intended to provide time series of surface heights for land-ice and
341 ice-shelf locations where ICESat-2 operates in repeat-track mode (*i.e.* for polar ice), along with
342 parameters useful in determining whether each height estimate is valid or a result of a variety of
343 potential errors (see ATL06 ATBD, section 1).

344 ATL11 height estimates are generated by correcting ATL06 height measurements for the
345 combined effects of short-scale (40-120-m) surface topography around the fit centers and small
346 (up to 130-m) horizontal offsets between repeat measurements. We fit a polynomial reference
347 surface to height measurements from different cycles as a function of horizontal coordinates
348 around the fit centers, and use this polynomial surface to correct the height measurements to the
349 fit center. The resulting values reflect the time history of surface heights at the reference points,
350 with minimal contributions from small-scale local topography.

351 In this algorithm, for a set of reference points spaced every 60 meters along each RPT (centered
352 on every third segment center), we consider all ATL06 segments with centers within 60 m along-
353 track and 65 m across-track of the reference point, so that each ATL11 fit contains as many as
354 seven distinct along-track segments from each laser beam and cycle. We select a subset of these
355 segments with consistent ATL06 slope estimates and small error estimates, and use these
356 segments to define a time-variable surface height and a polynomial surface-shape model. We
357 then use the surface-shape model to calculate corrected heights for the segments from cycles not
358 included in the initial subset. We propagate errors for each of these steps to give formal errors
359 estimates that take into account the sampling error from ATL06, and propagate the geolocation
360 errors with the slope of the surface-shape model to give an estimate of systematic errors in the
361 height estimates.
362

Figure 3-1. ATL11 fitting schematic



Schematic of the ATL11 fitting strategy. A and B show different renderings of the same set of data, A in perspective view and B from along the y (along-track axis). Lines show simulated ATL11 profiles; symbols show segment centers for segments within 60 m of the fit center (at $x=y=0$). Red lines and symbols indicate left beams, blue indicate right beams. 'o' markers indicate valid data segments, 'x' markers indicate invalid data segments. We plot the unperturbed, true surface height as a light-colored semi-transparent mesh, and the recovered surface height as a gray-shaded, opaque surface, shifted vertically to match the true surface. The gray surface shows the fit correction surface, offset vertically to match the true surface. C shows the uncorrected heights as a function of cycle number, and D shows the corrected heights (bottom), plotted for each repeat.

363
364

Figure 3-1. ATL11 fitting schematic

365 shows a schematic diagram of the fitting process. In this example, we show simulated ATL06
366 height measurements for six 91-day orbital cycles over a smooth ice-sheet surface (transparent
367 grid). Between cycles 3 and 4, the surface height has risen by 2 m. Two of the segments contain
368 errors: The weak beam for one segment from repeat 3 is displaced downward and has an
369 abnormal apparent slope in the x direction, and one segment from repeat 5 is displaced upwards,
370 so that its pair has an abnormal apparent slope in the y direction. Segments falling within the
371 across and along-track windows of the reference point (at $x=y=0$ in this plot) are selected, and fit
372 with a polynomial reference surface (shown in gray). When plotted as a function of cycle
373 number (panel C), the measured heights show considerable scatter but when corrected to the
374 reference surface (panel D), each cycle shows a consistent height, and the segments with errors
375 are clearly distinct from the accurate measurements.

376 3.1 Input data editing

377 Each ATL06 measurement includes location estimates, along- and across-track slope estimates,
378 and PE (Photon-Event)-height misfit estimates. To calculate the reference surface using the most
379 reliable subset of available data, we perform tests on the surface-slope estimates and error
380 statistics from each ATL06-pair to select a self-consistent set of data. These tests determine
381 whether each pair of measurements is *valid* and can be used in the reference-shape calculation or
382 is *invalid*. Segments from invalid pairs may be used in elevation-change calculations, but not in
383 the reference-shape calculation.

384 A complete flow chart of the data-selection process is shown in

Figure 3-2. Data selection

385 , and the parameters used to make these selections and their values are listed in Table 3-1.

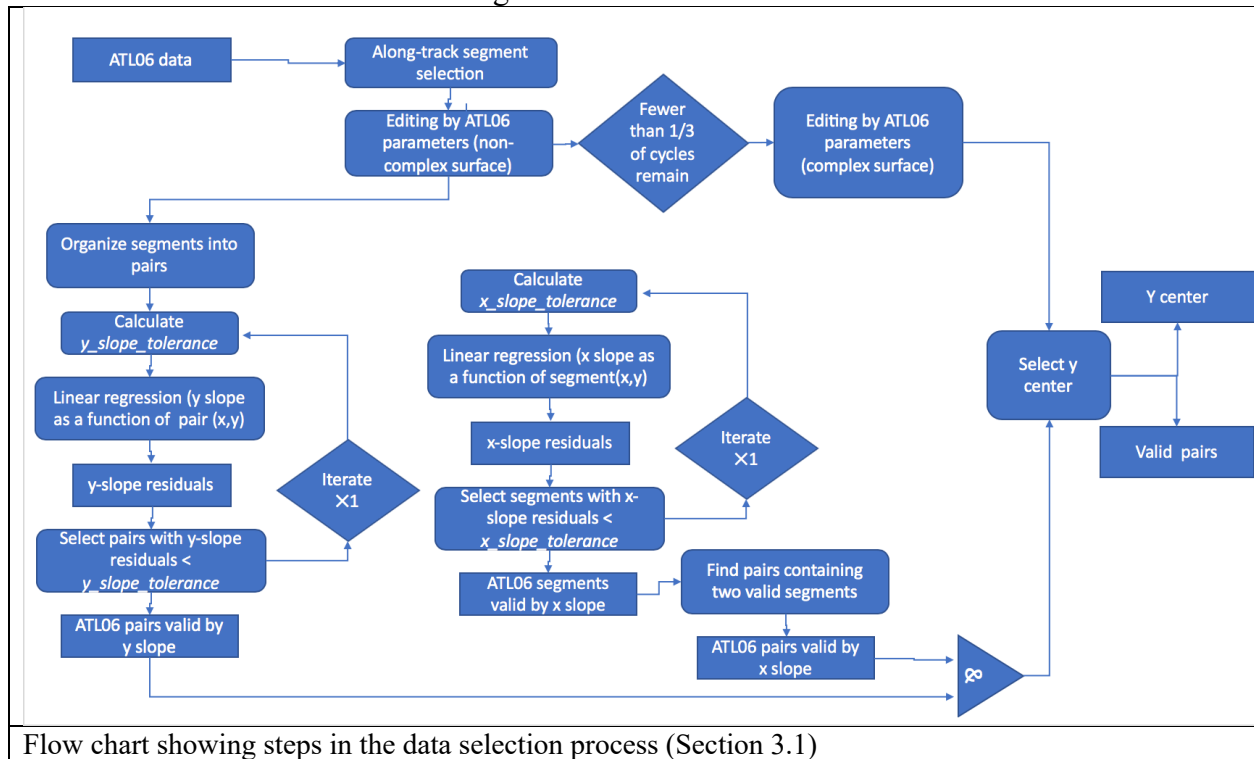
386

387 **Table 3-1 Parameter Filters to determine the validity of segments for ATL11 estimates**

complex_surface_flag	Segment parameter	Filter strategy	Section
0	<i>ATL06_quality_summary</i>	<i>ATL06_quality_summary</i> =0 (indicates high-quality segments)	3.1.1
1	<i>SNR_significance</i>	<i>SNR_significance</i> < 0.02 (indicates low probability of surface-detection blunders)	3.1.1
0 or 1	Along-track differences	Minimum height difference between the endpoints of a segment and the middles of its neighbors must be < 2 m (for smooth surfaces) or < 10 m (for complex surfaces)	3.1.1
0 or 1	<i>h_li_sigma</i>	<i>h_li_sigma</i> < max(0.05, 3*median(<i>h_li_sigma</i>))	3.1.1
0 or 1	Along-track slope	<i>r_slope_x</i> < 3 <i>slope_tolerance_x</i>	3.1.2
0 or 1	Across-track slope	<i>r_slope_y</i> < 3 <i>slope_tolerance_y</i>	3.1.2
0 or 1	Segment location	<i>x_atc-x0</i> < <i>L_search_XT</i> <i>y_atc-y0</i> < <i>L_search_AT</i>	3.1.3

388

Figure 3-2. Data selection



389

390 3.1.1 Input data editing using ATL06 parameters

391 For each reference point, we collect all ATL06 data from all available repeat cycles that have
 392 *segment_id* values within ± 3 of the reference point (inclusive) and that are on the same *rgt* and
 393 pair track as the reference point. The *segment_id* criterion ensures that the segment centers are
 394 within ± 60 m of the reference point in the along-track direction. We next check that the ATL06
 395 data are close to the pre-defined reference track, by rejecting all ATL06 segments that are more
 396 than 500 m away from the nominal pair across-track coordinates (-3200, 0, and 3200 meters for
 397 right, center, and left pairs, respectively). This removes data that were intentionally or
 398 accidentally collected with ATLAS pointed off nadir (i.e. for calibration scan maneuvers).

399 ATL06 contains some segments with signal-finding blunders (Smith et al., 2019). To avoid
 400 having these erroneous segments contaminate ATL11, we filter using one of two sets of tests,
 401 depending on surface roughness. We identify high-quality ATL06 segments, using parameters
 402 that depend on whether the surface is identified as smooth or rough, as follows:

403 1) For smooth ice-sheet surfaces, we use the ATL06 *ATL06_quality_summary* parameter,
 404 combined with a measure of along-track elevation consistency, *at_min_dh*, that is calculated as
 405 part of ATL11. *ATL06_quality_summary* is based on the spread of the residuals for each
 406 segment, the along-track surface slope, the estimated error, and the signal strength. Zero values
 407 indicate that no error has been found. We define the along-track consistency parameter
 408 *at_min_dh* as the minimum absolute difference between the heights of the endpoints of each
 409 segment and the center heights of the previous and subsequent segments. Its value will be small
 410 if a segment's height and slope are consistent with at least one of its neighbors. For smooth

411 surfaces, we require that the *at_min_dh* values be less than 2 m. Over smooth ice-sheet surfaces,
 412 the 2-m threshold eliminates most blunders without eliminating a substantial number of high-
 413 quality data points.

414 2) For rough, crevassed surfaces, the smooth-ice strategy may not identify a sufficient number of
 415 pairs for ATL11 processing to continue. If fewer than one third of the original cycles remain
 416 after the smooth-surface criteria are applied, we relax our criteria, using the signal-to-noise ratio
 417 (based on the ATL06 *segment_stats/snr_significance* parameter) to select the pairs to include in
 418 the fit, and require that the *at_min_dh* values be less than 10 m. If we relax the criteria in this
 419 way, we mark the reference point as having a complex surface using the
 420 *ref_surf/complex_surface_flag*, which limits the degree of the polynomial used in the reference
 421 surface fitting to 0 or 1 in each direction.

422 For either smooth or rough surfaces, we perform an additional check using the magnitude of
 423 *h_li_sigma* for each segment. If any segment's value is larger than three times the maximum of
 424 0.05 m and the median *h_li_sigma* for the valid segments for the current reference point, it is
 425 marked as invalid. The limiting 0.05 m value prevents this test from removing high-quality data
 426 over smooth ice-sheet surfaces, where errors are usually small.

427 Each of these tests applies to values associated with ATL06 segments. When the tests are
 428 complete, we check each ATL06 pair (*i.e.* two segments for the same along-track location from
 429 the same cycle) and if either of its two segments has been marked as invalid, the entire pair is
 430 marked as invalid.

431 3.1.2 Input data editing by slope

432 The segments selected in 3.1.1 may include some high-quality segments and some lower-quality
 433 segments that were not successfully eliminated by the data-editing criteria. We expect that the
 434 ATL06 slope fields (*dh_fit_dx*, and *dh_fit_dy*) for the higher-quality data should reflect the
 435 shape of an ice-sheet surface with a spatially consistent surface slope around each reference
 436 point, but that at least some of lower-quality data should have slope fields that outliers relative to
 437 this consistent surface slope. In this step, we assume that the slope may vary linearly in *x* and *y*,
 438 and so use residuals between the slope values and a regression of the slope values against *x* and *y*
 439 to identify the data with inconsistent slope values. The data with large residuals are marked as
 440 *invalid*.

441 Starting with valid pairs from 3.2.1, we first perform a linear regression between the *y* slopes of
 442 the pairs and the pair-center *x* and *y* positions. The residuals to this regression define one
 443 *y_slope_residual* for each pair. We compare these residuals against a *y_slope_tolerance*:

$$y_slope_tolerance = \max(0.01, 3 \text{ median } (dh_fit_dy_sigma), 3 \text{ RDE } (y_slope_residuals)) \quad 1$$

444 Here RDE is the Robust Difference Estimator, equal to half the difference between the 16th and
 445 84th percentiles of a distribution, and the minimum value of 0.01 ensures that this test does not
 446 remove high-quality segments in regions where the residuals are very consistent. If any pairs
 447 have a *y_slope_residual* greater than *y_slope_tolerance*, we remove them from the group of valid
 448 pairs, then repeat the regression, recalculate *y_slope_tolerance*, and retest the remaining pairs.
 449 We then return to the pairs marked as *valid* from 3.1.1, and perform a linear regression between
 450 the *x* slopes of the segments within the pairs and the segment-center *x* and *y* positions. The
 451 residuals to this regression define one *x_slope_residual* for each segment. We compare these

452 residuals against an $x_slope_tolerance$, calculated in the same way as (1), except using segment x
 453 slopes and residuals instead of pair y slopes. As with the y regression, we repeat this procedure
 454 once if any segments are eliminated in the first round.
 455 After both the x and y regression procedures are complete, each pair of segments is marked as
 456 *valid* if both of its x residuals are smaller than $slope_tolerance_x$ and its y residual is smaller than
 457 $slope_tolerance_y$.

458 3.1.3 Spatial data editing

459 The data included in the reference-surface fit fall in a “window” defined by a $2L_{search\ XT}$ by
 460 $2L_{search\ AT}$ rectangle, centered on each reference point. Because the across-track location of the
 461 repeat measurements for each reference point are determined by the errors in the repeat track
 462 pointing of ATLAS, a data selection window centered on the RPT in the y direction will not
 463 necessarily capture all of the available cycles of data. To improve the overlap between the
 464 window and the data, we shift the reference point in the y direction so that the window includes
 465 as many valid beam pairs as possible. We make this selection after the parameter-based (3.1.1)
 466 and slope-based (3.1.2) editing steps because we want to maximize the number high-quality pairs
 467 included, without letting the locations of low-quality segments influence our choice of the
 468 reference-point shift.

469 We select the across-track offset for each reference point by searching a range of offset values, δ ,
 470 around the RPT to maximize the following metric:

$$M(\delta) = \frac{[number\ of\ unique\ valid\ pairs\ entirely\ contained\ in\ \delta \pm L_{search\ XT}] + [number\ of\ unpaired\ segments\ contained\ in\ \delta \pm L_{search\ XT}]/100}{2}$$

471 Maximizing this metric allows the maximum number of pairs with two valid segments to be
 472 included in the fit, while also maximizing the number of segments included close to the center of
 473 the fit. If multiple values of δ have the same M value we choose the median of those δ values.

474 The across-track coordinate of the adjusted reference point is then $y_0 + \delta_{max}$, where y_0 is the
 475 across-track coordinate of the unperturbed reference point. After this adjustment, the segments
 476 in pairs that are contained entirely in the across-track interval $\delta \pm L_{search\ XT}$ are identified as
 477 *valid* based on the spatial search.

478 The location of the adjusted reference point is reported in the data group for each pair track, with
 479 corresponding local coordinates in the *ref_surf* subgroup: */ptx/ref_surf/x_atc*, */ptx/ref_surf/y_atc*.

481 3.2 Reference-Surface Shape Correction

482 To calculate the reference-surface shape correction, we construct the background surface shape
 483 from valid segments selected during 3.1 and 3.2, using a least-squares inversion that separates
 484 surface-shape information from elevation-change information. This produces surface shape-
 485 corrected height estimates for cycles containing at least one valid pair, and a surface-shape
 486 model that we use in later steps (3.4, 3.6) to calculate corrected heights for cycles that contain no
 487 valid pairs and to calculate corrected heights for crossing tracks.

488 **3.2.1 Reference-surface shape inversion**

489 The reference-shape inversion solves for a reference surface and a set of corrected-height values
 490 that represent the time-varying surface height at the reference point. The inversion involves
 491 three matrices:

492 (i): a polynomial surface shape matrix, **S**, that describes the functional basis for the spatial part of
 493 the inversion:

$$\mathbf{S} = \left[\left(\frac{x - x_0}{l_0} \right)^p \left(\frac{y - y_0}{l_0} \right)^q \right] \quad 3$$

494 Here x_0 and y_0 are equal to the along-track coordinates of the adjusted reference point,
 495 */ptx/ref_surf/x_atc* and */ptx/ref_surf/y_atc*, respectively. **S** has one column for each permutation
 496 of p and q between zero and the degree of the surface polynomial in each dimension, but does
 497 not include a $p=q=0$ term. The degree is chosen to be no more than 3 (in the along-track
 498 direction) or 2 (in the across-track direction), and to be no more than the number of distinct pair-
 499 center y values (in the across-track direction) or more than 1 less than the number of distinct x
 500 values (in the along-track direction) in any cycle, with distinct values defined at a resolution of
 501 20 m in each direction. The scaling factor, l_0 , ensures that the components of **S** are on the order
 502 of 1, which improves the numerical accuracy of the computation. We set $l_0=100$ m, to
 503 approximately match the intra-pair beam spacing.

504 (ii): a matrix that encodes the repeat structure of the data, that accounts for the height-change
 505 component of the inversion:

$$\mathbf{D} = [\delta(i, 1), \delta(i, 2), \dots, \delta(i, N)] \quad 4$$

506 Here δ is the delta function, equal to 1 when its arguments are equal, zero otherwise, and i is an
 507 index that increments by one for each distinct cycle in the selected data.

508 (iii): a matrix that describes the linear rate of change in the surface slope over the course of the
 509 mission:

$$\mathbf{S}_t = \left[\left(\frac{x - x_0}{l_0} \right) \left(\frac{t - t_0}{\tau} \right), \left(\frac{y - y_0}{l_0} \right) \left(\frac{t - t_0}{\tau} \right) \right] \quad 5$$

510 Here t_0 is equal to *slope_change_t0*, the mid-point of the mission at the time that ATL11 is
 511 generated, halfway between start repeat track pointing (the beginning of cycle 3) and either the
 512 end of the mission or the processing time (*slope_change_t0* is an attribute of each ATL11
 513 file). This implies that on average, $(t - t_0)$ will have a zero mean. The time-scaling factor, τ , is
 514 equal to one year (86400*365.25 seconds). This component will only be included in ATL11
 515 once eight complete cycles of data are available on the RGTs (after cycle 10 of the mission).
 516 The surface shape, slope change, and height time series are estimated by forming a composite
 517 design matrix, **G**, where

$$\mathbf{G} = [\mathbf{S} \ \mathbf{S}_t \ \mathbf{D}], \quad 6$$

518 and a covariance matrix, **C**, containing the squares of the segment-height error estimates on its
 519 diagonal. The surface-shape polynomial and the height changes are found:

$$\begin{aligned} [\mathbf{s}, \mathbf{s}_t, \mathbf{z}_c] &= \mathbf{G}^{-\mathbf{g}} \mathbf{z} \\ \text{where} & \\ \mathbf{G}^{-\mathbf{g}} &= [\mathbf{G}^T \mathbf{C}^{-1} \mathbf{G}]^{-1} \mathbf{G}^T \mathbf{C}^{-1} \end{aligned} \quad 7$$

520 The notation $[\]^{-1}$ designates the inverse of the quantity in brackets, and \mathbf{z} is the vector of segment
 521 heights. The parameters derived in this fit are \mathbf{s} , a vector of surface-shape polynomial
 522 coefficients, \mathbf{s}_t , the mean rate of surface-slope change, and \mathbf{z}_c , a vector of corrected height values,
 523 giving the height at (lat_0, lon_0) as inferred from the height measurements and the surface
 524 polynomial. The matrix $\mathbf{G}^{\#}$ is the generalized inverse of \mathbf{G} . The values of \mathbf{s} are reported in the
 525 *ref_surf/poly_ref_surf* parameter, as they are calculated from (6), with no correction made for the
 526 scaling in (3). The values for the slope-change rates are reported in *ref_surf/slope_change_rate*,
 527 after rescaling to units of *years⁻¹*.

528 3.2.2 Misfit analysis and iterative editing

529 If blunders remain in the data input to the reference-surface calculation, they can lead to
 530 inaccurate reference surfaces. To help remove these blunders, we iterate the inversion procedure
 531 in 3.2.1, eliminating outlying data points based on their residuals to the reference surface.
 532 To determine whether outliers may be present, we calculate the chi-squared misfit between the
 533 data and the fit surface based on the data covariance matrix and the residual vector, r :

$$\chi^2 = r^T \mathbf{C}^{-1} r \quad 8$$

534 To determine whether this misfit statistic indicates consistency between the polynomial surface
 535 and the data we use a P statistic, which gives the probability that the given χ value would be
 536 obtained from a random Gaussian distribution of data points with a covariance matrix \mathbf{C} . If the
 537 probability is less than 0.025, we perform some further filtering/editing: we calculate the RDE of
 538 the scaled residuals, eliminate any pairs containing a segment whose scaled residual magnitude is
 539 larger than three times that value, and repeat the remaining segments.

540 After each iteration, any column of \mathbf{G} that has a uniform value (i.e. all the values are the same) is
 541 eliminated from the calculation, and the corresponding value of the left-hand side of equation 7
 542 is set to zero. Likewise, if the inverse problem has become less than overdetermined (i.e., the
 543 number of data is smaller than the number of unknown values they are constraining), the
 544 polynomial columns of \mathbf{G} are eliminated one by one until the number of data is greater than the
 545 number of unknowns. Columns are eliminated in descending order of the sum of x and y
 546 degrees, and when there is a tie between columns based on this criterion, the column with the
 547 larger y degree is eliminated first.

548 This fitting procedure is continued until no further segments are eliminated. If more than three
 549 complete cycles that passed the initial editing steps are eliminated in this way, the surface is
 550 assumed to be too complex for a simple polynomial approximation, and we proceed as follows:

551 (i) the fit and its statistics are reported based on the complete set of pairs that passed
 552 the initial editing steps (valid pairs), using a planar ($x_degree = y_degree = 1$) fit in x and y .

553 (ii) the *ref_surf/complex_surface_flag* is set to 1.

554 The misfit parameters are reported in the *ref_surf* group: The final chi-squared statistic is
 555 reported as *ref_surf/misfit_chi2r*, equal to the chi-squared statistic divided by the number of
 556 degrees of freedom in the solution; the final RMS of the scaled residuals is reported as
 557 *ref_surf/misfit_rms*.

558 3.3 Reference-shape Correction Error Estimates

559 We first calculate the errors in the corrected surface heights for segments included in the
 560 reference-surface fit. We form a second covariance matrix, \mathbf{C}_1 , whose diagonal elements are the
 561 maximum of the squares of the segment errors and $\langle r^2 \rangle$. We estimate the covariance matrix for
 562 the height estimates:

$$\mathbf{C}_m = \mathbf{G}^{-g} \mathbf{C}_1 \mathbf{G}^{-gT} \quad 9$$

563 The square roots of the diagonal values of \mathbf{C}_m give the estimated errors in the surface-polynomial
 564 and height estimates due to short-spatial-scale errors in the segment heights. If there are N_{coeff}
 565 coefficients in the surface-shape polynomial, and $N_{shape-cycles}$ cycles included in the surface-shape
 566 fit, then the first N_{coeff} diagonal elements of \mathbf{C}_m give the square of the errors in the surface-shape
 567 polynomial and the last $N_{shape-cycles}$ give the errors in the surface heights for the cycles included in
 568 the fit. The portion of \mathbf{C}_m that refers only to the surface shape and surface-shape change
 569 components is $\mathbf{C}_{m,s}$.

570 3.4 Calculating corrected height values for repeats with no selected pairs

571 Once the surface polynomial has been established from the edited data set, corrected heights are
 572 calculated for the unselected cycles (*i.e.* those from which all pairs were removed in the editing
 573 steps): For the segments among these cycles, we form a new surface and slope-change design
 574 matrix, $[\mathbf{S}, \mathbf{S}_t]$ and multiply it by $[\mathbf{s}, \mathbf{s}_t]$ to give the surface-shape correction:

$$\mathbf{z}_c = \mathbf{z} - [\mathbf{S}, \mathbf{S}_t][\mathbf{s}, \mathbf{s}_t] \quad 10$$

575 Here \mathbf{s} is the surface-shape polynomial, and \mathbf{s}_t is the slope-change-rate estimate. This gives up to
 576 fourteen corrected-height values per unselected cycle. From among these, we select the segment
 577 with the minimum error, as calculated in the next step.

578 The height errors for segments from cycles not included in the surface-shape fit are calculated:

$$\sigma_{z,c}^2 = \text{diag}([\mathbf{S}, \mathbf{S}_t] \mathbf{C}_{m,s} [\mathbf{S}, \mathbf{S}_t]^T) + \sigma_z^2 \quad 11$$

579 Here σ_z is the error in the segment height, and $\sigma_{z,c}$ is the error in the corrected height. The
 580 results of these calculations give a height and a height error for each unselected segment. To
 581 obtain a corrected elevation for each repeat that contains no selected pairs, we identify the
 582 segment from that repeat that has the smallest error estimate, and report the value z_c as that
 583 repeat's *ptx/h_corr*, and use $\sigma_{z,c}$ as its error (*/ptx/h_corr_sigma*).

584 3.5 Calculating systematic error estimates

585 The errors that have been calculated up to this point are due to errors in fitting segments to
 586 photon-counting data and due to inaccuracies in the polynomial fitting model. Additional error
 587 components can result from more systematic errors, such as errors in the position of ICESat-2 as
 588 derived from POD, and pointing errors from PPD. These are estimated in the ATL06
 589 *sigma_geo_xt*, *sigma_geo_at*, and *sigma_geo_r* parameters, and their average for each repeat is
 590 reported in the *cycle_stats* group under the same parameter names. The geolocation component
 591 of the total height is the product of the geolocation error and the surface slope, added in
 592 quadrature with the vertical height error:

$$\sigma_{h,systematic} = \left[\left(\frac{dh}{dx} \sigma_{geo,AT} \right)^2 + \left(\frac{dh}{dy} \sigma_{geo,XT} \right)^2 + \sigma_{geo,r}^2 \right]^{1/2} \quad 12$$

593 For selected segments, which generally come from pairs containing two high-quality height
 594 estimates, dh/dy is estimated from the ATL06 dh_fit_dy parameter. For unselected segments, it is
 595 based on the y component of the reference-surface slope, as calculated in section 4.2.
 596 The error for a single segment's corrected height is:

$$\sigma_{h,total} = [\sigma_{h,systematic}^2 + \sigma_{h,c}^2]^{1/2} \quad 13$$

597 This represents the total error in the surface height for a single corrected height. In most cases,
 598 error estimates for averages of ice-sheet quantities will depend on errors from many segments
 599 from different reference points, and the spatial scale of the different error components will need
 600 to be taken into account in error propagation models. To allow users to separate these effects,
 601 we report both the uncorrelated error, $/ptx/h_corr_sigma$, and the component due only to
 602 systematic errors, $/ptx/h_corr_sigma_systematic$. The total error is the quadratic sum of the two,
 603 as described in equation 13.

604 3.6 Calculating shape-corrected heights for crossing-track data

605 Locations where groundtracks cross provide opportunities to check the accuracy of
 606 measurements by comparing surface-height estimates between the groundtracks, and also offers
 607 the opportunity to generate elevation-change time series that have more temporal detail than the
 608 91-day repeat cycle can offer for repeat-track measurements.

609 At these crossover points, we use the reference surface calculated in 3.5 to calculate corrected
 610 elevations for the crossing tracks. We refer to the track for which we have calculated the
 611 reference surface as the *datum* track, and the other track as the *crossing* track. To calculate
 612 corrected surface heights for the crossing ICESat-2 orbits, we first select all data from the
 613 crossing orbit within a distance L_search_XT of the updated reference point on the datum track.
 614 For most datum reference points, this will yield no crossing data, in which case the calculation
 615 for that datum point terminates. If crossing data are found, we then calculate the coordinates of
 616 these points in the reference point's along-track and across-track coordinates. This calculation
 617 begins by transforming the crossing-track data into local northing and easting coordinates
 618 relative to the datum reference-point location:

$$\delta N_c = \frac{\pi R_e}{180} (lat_c - lat_d) \quad 14$$

$$\delta E_c = \frac{\pi R_e}{180} (lon_c - lon_d) \cos(lat_c)$$

619 Here (lat_d, lon_d) are the coordinates of the adjusted datum reference point, (lat_c, lon_c) are the
 620 coordinates of the points on the crossing track, and R_e is the local radius of the WGS84 ellipsoid.
 621 We then convert the northing and easting coordinates into along-track and across-track
 622 coordinates based on the azimuth ϕ of the datum track:

$$\begin{aligned} x_c &= \delta N_c \cos(\phi) + \delta E_c \sin(\phi) \\ y_c &= \delta N_c \sin(\phi) - \delta E_c \cos(\phi) \end{aligned} \quad 15$$

623 Using these coordinates, we proceed as we did in 3.4 and 3.5: we generate S_k and S_{kt} matrices,
 624 use them to correct the data and to identify the data point with the smallest error for each
 625 crossing cycle. We report the time, error estimate, and corrected height for the minimum-error
 626 datapoint from each cycle, as well as the location, pair, and track number corresponding to the
 627 datum point in the `/ptx/crossing_track_data` group. Because the crossing angles between the
 628 tracks are oblique at high latitudes, a particular crossing track may appear in a few subsequent
 629 datum points; in these cases, we expect that the error estimates should vary with the distance
 630 between the crossing track and the datum track, so that the point with the minimum error should
 631 correspond to the precise crossing location of the two tracks.

632 To help evaluate the quality of crossing-track data we calculate the `along_track_rss` parameter
 633 for each crossing-track measurement. This parameter gives the RSS of the differences between
 634 each segment's endpoint heights and the heights of the previous and subsequent segments. A
 635 segment that is consistent with the previous and next segments in slope and elevation will have a
 636 small value for this parameter, a segment that is inconsistent (and thus potentially in error) will
 637 have a large value. Crossing-track measurements that have values greater than 10 m are
 638 excluded from ATL11 and do not appear in the dataset.

639 3.7 Calculating parameter averages

640 ATL11 contains a variety of parameters that mirror parameters in ATL06, but are averaged to the
 641 140-m ATL11 resolution. Except where noted otherwise, these quantities are weighted averages
 642 of the corresponding ATL06 values. For selected pairs (i.e. those included in the reference-
 643 surface fit), the parameters are averaged over the selected segments from each cycle, using
 644 weights derived from their formal errors, h_li_sigma . The parameter weighted average for the N_k
 645 segments from cycle k is then:

$$\langle q \rangle = \frac{\sum_{i=1}^{N_k} |\sigma_i^{-2}| q_i}{\sum_{i=1}^{N_k} |\sigma_i^{-2}|} \quad 16$$

646 Here q_i are the parameter values for the segments. For repeats with no selected pairs, recall that
 647 the corrected height for only one segment is reported in `/ptx/h_corr`; for these, we simply report
 648 the corresponding parameter values for that selected segment.
 649

650 3.8 Output data editing

651 The output data product includes cycle height estimates only for those cycles that have
 652 non-systematic error estimates (`/ptx/h_corr_sigma`) less than 15 m. All other heights (and their
 653 errors) are reported as *invalid*.
 654

655

656 **4.0 LAND ICE PRODUCTS: LAND ICE H(T) (ATL 11/L3B)**

657 Each ATL11 file contains data for a single reference ground track, for one of the subregions
658 defined for ATLAS granules (see

Figure 6-3. Granule regions

659). The ATL11 consists of three top-level groups, one for each beam pair (*pt1*, *pt2*, *pt3*). Within
 660 each pair-track group, there are datasets that give the corrected heights for each cycle, their
 661 errors, and the reference-point locations. Subgroups (*cycle_stats*, and *ref_surf*) provide a set of
 662 data-quality parameters, and ancillary data describing the fitting process, and use the same
 663 ordering and coordinates as the top-level group (i.e. any dataset within the */ptx/cycle_stats* and
 664 */ptx/ref_surf* groups refers to the same latitude, longitude, and reference points as the
 665 corresponding measurements in the */ptx/* groups.) The *crossing_track_data* group gives height
 666 measurements at crossover locations, and has its own set of locations and
 667

668 4.1 File naming convention

669 ATL11 files are named in the following format:

670 `ATL11_ttttgg_cccc_rrr_vv.h5`

671 Here *tttt* is the rgt number, *gg* is the granule-region number, *cccc* gives the first and last cycles of
 672 along-track data included in the file (e.g. `_0308_` would indicate that cycles three through eight,
 673 inclusive, might be included in the along-track solution), and *rrr* is the release number. and *vv* is
 674 the version number, which is set to one the first time a granule is generated for a given data
 675 release, and is incremented by one if the granule is regenerated.
 676

677 4.2 */ptx* group

678
 679 Table 4-1 shows the datasets in the *ptx* groups. This group gives the principal output parameters
 680 of the ATL11. The corrected repeat measurements are in */ptx/h_corr*, which gives improved
 681 height measurements based on a surface fit to valid data at paired segments. The associated
 682 reference coordinates, */ptx/latitude* and */ptx/longitude* give the reference point location, with
 683 averaged times per repeat, */ptx/delta_time*. For repeats with no selected pairs, the corrected
 684 height is that from the selected segment with the lowest error. Two error metrics are given in
 685 */ptx/h_corr_sigma* and */ptx/h_corr_sigma_systematic*. The first gives the error component due to
 686 ATL06 range errors and due to uncertainty in the reference surface. The second gives the
 687 component due to geolocation and radial-orbit errors that are correlated at scales larger than one
 688 reference point; adding these values in quadrature gives the total per-cycle error. Values are only
 689 reported for */ptx/h_corr*, */ptx/h_corr_sigma*, and */ptx/h_corr_sigma_systematic* for those cycles
 690 whose uncorrelated errors are less than 15 m; all others are reported as *invalid*. A
 691 */ptx/quality_summary* is included for each cycle, based on fit statistics from ATL06.

692

693

Table 4-1 Parameters in the /ptx/ group

Parameter	Units	Dimensions	Description
<i>cycle_number</i>	counts	$I \times N_{cycles}$	Cycle number for each column of the data
<i>latitude</i>	degrees North	$N_{pts} \times I$	Reference point latitude
<i>longitude</i>	degrees East	$N_{pts} \times I$	Reference point longitude
<i>ref_pt</i>	counts	$N_{pts} \times I$	The reference point number, <i>m</i> , counted from the equator crossing of the RGT.
<i>delta_time</i>	seconds	$N_{pts} \times N_{cycles}$	mean GPS time for the segments for each cycle
<i>h_corr</i>	meters	$N_{pts} \times N_{cycles}$	the mean corrected height
<i>h_corr_sigma</i>	meters	$N_{pts} \times N_{cycles}$	the formal error in the corrected height
<i>h_corr_sigma_systematic</i>	meters	$N_{pts} \times N_{cycles}$	the magnitude of the RSS of all errors that might be correlated at scales larger than a single reference point (e.g. pointing errors, GPS errors, etc)
<i>quality_summary</i>	counts	$N_{pts} \times N_{cycles}$	summary flag: zero indicates high-quality cycles: where $\min(\text{signal_selection_source}) \leq 1$ and $\min(\text{SNR_significance}) < 0.02$, and $\text{ATL06_summary_zero_count} > 0$.

694

695 **4.3 /ptx/ref_surf group**

696 Table 4-2 describes the /ptx/ref_surf group. This group includes parameters describing the
 697 reference surface fit at each reference point. The polynomial coefficients are given in
 698 /ptx/poly_ref_surf, sorted first by total degree, then by x-component degree. Because the

699 polynomial degree is chosen separately for each reference point, enough columns are provided in
 700 the */ptx/poly_ref_surf* and */ptx/poly_ref_surf_sigma* to accommodate all possible components up
 701 to 2rd degree in *y* and 3th degree in *x*, and absent values are filled in with zeros. The
 702 correspondence between the columns of the polynomial fields and the exponents of the *x* and *y*
 703 terms are given in the */ptx/poly_exponent_x* and */ptx/poly_exponent_y* fields. The time origin for
 704 the slope change is given in the group attribute */ptx/slope_change_t0*.

Table 4-2 Parameters in the */ptx/ref_surf* group

Parameter	Units	Dimensions	Description
<i>dem_h</i>	Meters	$N_{pts} \times 1$	DEM elevation, derived from the ATL06 <i>dem_h</i> parameter
<i>geoid_h</i>	Meters	$N_{pts} \times 1$	Geoid height above WGS-84 reference ellipsoid in the tide-free system, derived from ATL06 <i>/gtxx/atl06_segments/dem/geoid_h</i>
<i>complex_surface_flag</i>	counts	$N_{pts} \times 1$	0 indicates that normal fitting was attempted, 1 indicates that the signal selection algorithm rejected too many repeats, and only a linear fit was attempted
<i>rms_slope_fit</i>	counts	$N_{pts} \times 1$	the RMS of the slope of the fit polynomial within 50 m of the reference point
<i>e_slope</i>	counts	$N_{pts} \times 1$	the mean East-component slope for the reference surface within 50 m of the reference point
<i>n_slope</i>	counts	$N_{pts} \times 1$	the mean North-component slope for the reference surface within 50 m of the reference point
<i>at_slope</i>	Counts	$N_{pts} \times 1$	Mean along-track component of the slope of the reference surface within 50 m of the reference point
<i>xt_slope</i>		$N_{pts} \times 1$	Mean across-track component of the slope of the reference surface within 50 m of the reference point
<i>deg_x</i>	counts	$N_{pts} \times 1$	Maximum degree of non-zero polynomial components in <i>x</i>
<i>deg_y</i>	counts	$N_{pts} \times 1$	Maximum degree of non-zero polynomial components in <i>y</i>
<i>poly_exponent_x</i>	counts	1×8	Exponents for the <i>x</i> factors in the surface polynomial
<i>poly_exponent_y</i>	counts	1×8	Exponents for the <i>y</i> factors in the surface polynomial
<i>poly_coeffs</i>	counts	$N_{pts} \times 8$	polynomial coefficients (up to degree 3), for polynomial components scaled by 100 m

<i>poly_ref_coeffs_sigma</i>	counts	$N_{pts} \times 8$	formal errors for the polynomial coefficients
<i>ref_pt_number</i>	counts	$N_{pts} \times 1$	Ref point number, counted from the equator crossing along the RGT.
<i>x_atc</i>	meters	$N_{pts} \times 1$	Along-track coordinate of the reference point, measured along the RGT from its first equator crossing.
<i>y_atc</i>	meters	$N_{pts} \times 1$	Across-track coordinate of the reference point, measured along the RGT from its first equator crossing.
<i>rgt_azimuth</i>	degrees	$N_{pts} \times 1$	Reference track azimuth, in degrees east of local north
<i>slope_change_rate_x</i>	years ⁻¹	$N_{pts} \times 1$	rate of change of the x component of the surface slope
<i>slope_change_rate_y</i>	years ⁻¹	$N_{pts} \times 1$	rate of change of the y component of the surface slope
<i>slope_change_rate_x_sigma</i>	years ⁻¹	$N_{pts} \times 1$	Formal error in the rate of change of the x component of the surface slope
<i>slope_change_rate_y_sigma</i>	years ⁻¹	$N_{pts} \times 1$	Formal error in the rate of change of the y component of the surface slope
<i>misfit_chi2r</i>	meters	$N_{pts} \times 1$	misfit chi square, divided by the number of degrees in the solution
<i>misfit_rms</i>	meters	$N_{pts} \times 1$	RMS misfit for the surface-polynomial fit
<i>fit_quality</i>	counts	$N_{pts} \times 1$	Indicates quality of the fit: 0: no problem identified 1: One or more polynomial coefficient errors larger than 10 2: One or more components of the surface slope has magnitude larger than 0.2 3: Conditions 1 and 2 both true.

705
706
707
708
709
710
711
712
713
714
715
716

The slope of the fit surface is given in the *ref_surf/n_slope* and *ref_surf/e_slope* parameters in the local north and east directions; the corresponding slopes in the along-track and across-track directions are given in the *ref_surf/xt_slope* and *ref_surf/yt_slope* parameters. For the along-track points, the surface slope is calculated by evaluating the correction-surface polynomial for a 10-m spaced grid of points extending ± 50 m in x and y around the reference point, and calculating the mean slopes of these points. The calculation is performed in along-track coordinates and then projected onto the local north and east vectors. The *rms_slope_fit* is derived from the same set of points, and is calculated as the RMS of the standard deviations of the slopes calculated from adjacent grid points, in x and y.

717 **4.4 /ptx/cycle_stats group**

718 The /ptx/cycle_stats group gives summary information about the segments present for each
 719 reference point. Most parameters are averaged according to equation 14, but for others (e.g.
 720 /ptx/signal_selection_flag_best, which is the minimum of the signal selection flags for the cycle)
 721 **Table 4-3** describes how the summary statistics are derived.

722

723 **Table 4-3 Parameters in the /ptx/cycle_stats group**

Parameter	Units	Dimensions	Description
<i>ATL06_summary_zero_count</i>	counts	$N_{pts} \times N_{cycles}$	Number of segments with <i>atl06_quality_summary</i> =0 (0 indicates the best-quality data)
<i>h_rms_misfit</i>	meters	$N_{pts} \times N_{cycles}$	Weighted-average RMS misfit between PE heights and along-track land-ice segment fit
<i>r_eff</i>	counts	$N_{pts} \times N_{cycles}$	Weighted-average effective, uncorrected reflectance for each cycle.
<i>tide_ocean</i>	meters	$N_{pts} \times N_{cycles}$	Weighted-average ocean tide for each cycle
<i>dac</i>	meters	$N_{pts} \times N_{cycles}$	Dynamic atmosphere correction (mainly the effect of atmospheric pressure on floating-ice elevation).
<i>cloud_flg_atm</i>	counts	$N_{pts} \times N_{cycles}$	Minimum cloud flag from ATL06: Flag indicates confidence that clouds with $OT^* > 0.2$ are present in the lower 3 km of the atmosphere based on ATL09
<i>cloud_flg_asr</i>	counts	$N_{pts} \times N_{cycles}$	Minimum apparent-surface-reflectance - based cloud flag from ATL06: Flag indicates confidence that clouds with $OT > 0.2$ are present in the lower 3 km of the atmosphere based on ATL09
<i>bsnow_h</i>	meters	$N_{pts} \times N_{cycles}$	Weighted-average blowing snow layer height for each cycle
<i>bsnow_conf</i>	counts	$N_{pts} \times N_{cycles}$	Maximum <i>bsnow_conf</i> flag from ATL06: indicates the greatest (among segments) confidence flag for presence of blowing snow for each cycle

Parameter	Units	Dimensions	Description
<i>x_atc</i>	meters	$N_{pts} \times N_{cycles}$	weighted average of pair-center RGT y coordinates for each cycle
<i>y_atc</i>	meters	$N_{pts} \times N_{cycles}$	weighted mean of pair-center RGT y coordinates for each cycle
<i>ref_pt</i>		$N_{pts} \times N_{cycles}$	Ref point number, counted from the equator crossing along the RGT.
<i>seg_count</i>	counts	$N_{pts} \times N_{cycles}$	Number of segments marked as valid for each cycle. Equal to 0 for those cycles not included in the reference-surface shape fit.
<i>min_signal_selection_source</i>	counts	$N_{pts} \times N_{cycles}$	Minimum of the ATL06 <i>signal_selection_source</i> value (indicates the highest-quality segment in the cycle)
<i>min_snr_significance</i>	counts	$N_{pts} \times N_{cycles}$	Minimum of <i>SNR_significance</i> (indicates the quality of the best segment in the cycle)
<i>sigma_geo_h</i>	meters	$N_{pts} \times N_{cycles}$	Root-mean-weighted-square-average total vertical geolocation error due to PPD and POD
<i>sigma_geo_at</i>	meters	$N_{pts} \times N_{cycles}$	Root-mean-weighted-square-average local-coordinate x horizontal geolocation error for each cycle due to PPD and POD
<i>sigma_geo_xt</i>	meters	$N_{pts} \times N_{cycles}$	Root-mean-weighted-square-average local-coordinate y horizontal geolocation error for each cycle due to PPD and POD
<i>h_mean</i>	meters	$N_{pts} \times N_{cycles}$	Weighted-average of surface heights, not including the correction for the reference surface

724 *OT (optical thickness) is a measure of signal attenuation used in atmospheric calculations. This
 725 parameter discussed in ICESat-2 atmospheric products (ATL09)
 726

727 **4.5 /ptx/crossing_track_data group**

728 The /ptx/crossing_track_data group (Table 4-4) contains elevation data at crossover locations.
 729 These are locations where two ICESat-2 pair tracks cross, so data are available from both the
 730 datum track, for which the granule was generated, and from the crossing track. The data in this

731 group represent the elevations and times from the crossing tracks, corrected using the reference
 732 surface from the datum track. Each set of values gives the data from a single segment on the
 733 crossing track, that was selected as having the minimum error among all segments on the
 734 crossing track within the $2 L_{search_XT}$ -by- $2 L_{search_AT}$ window around the reference point
 735 on the datum track. The systematic errors are evaluated based on the magnitude of the reference-
 736 surface slope and the magnitude of the horizontal geolocation error of the crossing-track data.
 737 Attributes for the group specify the track number and pair-track number of the crossing track.
 738

Table 4-4 Parameters in the /ptx/crossing_track_data group

Parameter	Units	Dimensions	Description
<i>ref_pt</i>	counts	$N_{XO} \times I$	the reference-point number for the datum track
<i>delta_time</i>	years	$N_{XO} \times I$	time relative to the ICESat-2 reference epoch
<i>h_corr</i>	meters	$N_{XO} \times I$	WGS-84 height, corrected for the ATL11 surface shape
<i>h_corr_sigma</i>	meters	$N_{XO} \times I$	error in the height estimate
<i>h_corr_sigma_systematic</i>	meters	$N_{XO} \times I$	systematic error in the height estimate
<i>ocean_tide</i>	Meters	$N_{XO} \times I$	Ocean-tide estimate for the crossing track
<i>dac</i>	Meters	$N_{XO} \times I$	Dynamic atmosphere correction for the crossing track
<i>latitude</i>	degrees	$N_{XO} \times I$	latitude of the crossover point
<i>longitude</i>	degrees	$N_{XO} \times I$	longitude of the crossover point
<i>cycle_number</i>	counts	$N_{XO} \times I$	Cycle number for the crossing data
<i>rgt</i>	counts	$N_{XO} \times I$	The RGT number for the crossing data
<i>spot_crossing</i>	counts	$N_{XO} \times I$	The spot number for the crossing data
<i>atl06_quality_summary</i>	counts	$N_{XO} \times I$	quality flag for the crossing data derived from ATL06. 0 indicates no problems detected, 1 indicates potential problems
<i>along_track_rss</i>	meters	$N_{XO} \times I$	Root sum of the squared differences between the heights of the endpoints for the crossing-track segment and the centers of the previous and next segments

739

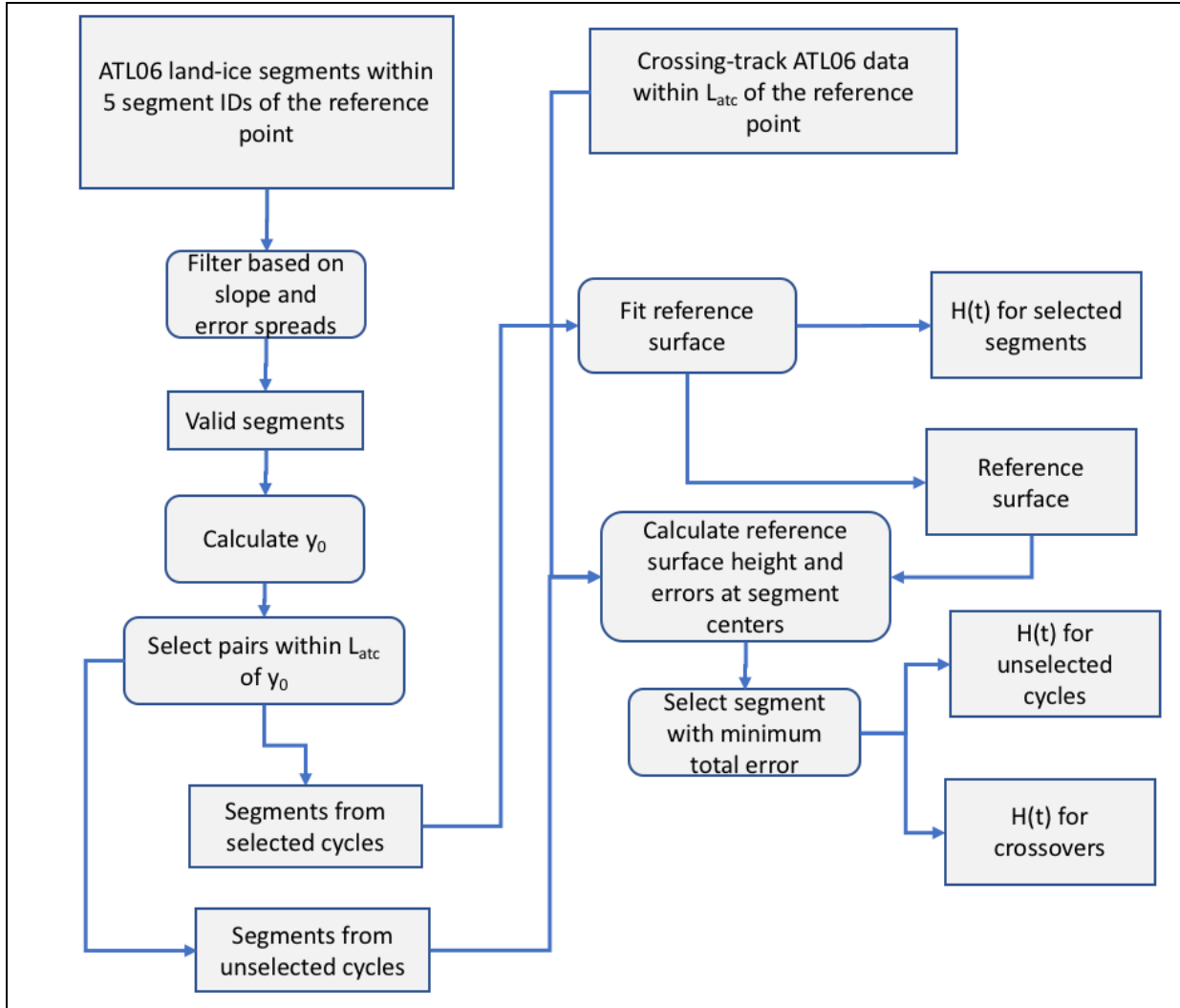
740

741 5.0 ALGORITHM IMPLEMENTATION

742

743

Figure 5-1 Flow Chart for ATL11 Surface-shape Corrections



744

745

746 The following steps are performed for each along-track reference point.

747

748

749

750

751

752

753

754

1. Segments with *segment_id* within $N_search/2$ of the reference-point number, are selected.
2. Valid segments are identified based on estimated errors, the *ATL06_quality_summary* parameter, and the along- and across-track segment slopes. Valid pairs, containing valid measurements from two different beams, are also identified.
3. The location of the reference point is adjusted to allow the maximum number of repeats with at least one valid pair to fall within the across-track search distance of the reference point.

- 755 4. The reference surface is fit to pairs with two valid measurements within the search
 756 distance of the reference point. This calculation also produces corrected heights for the
 757 selected pairs and the errors in the correction polynomial coefficients.
 758 5. The correction surface is used to derive corrected heights for segments not selected in
 759 steps 1-3, and the height for the segment with the smallest error is selected for each
 760 6. The reference surface is used to calculate heights for external (pre-ICESat-2) laser
 761 altimetry data sets and crossover ICESat-2 data.
 762 A schematic of this calculation is shown in Figure 5-1.

763 5.1.1 Select ATL06 data for the current reference point

764 **Inputs:**

- 765 *ref_pt*: segment number for the current reference point
 766 *track_num*: The track number for current point
 767 *pair_num*: The pair number for the current point

768 **Outputs:**

- 769 *D_ATL06*: ATL06 data structure

770 **Parameters:**

- 771 *N_search*: number of segments to search, around *ref_pt*, equal to 5.

772 **Algorithm:**

- 773 1. For each along-track point, load all ATL06 data from track *track_num* and pair *pair_num* that
 774 have *segment_id* within *N_search* of *ref_pt*: These segments have $ref_pt - N_search$
 775 $\leq segment_id \leq ref_pt + N_search$.
 776 2. Reject any data that have *y_atc* values more than 500 m distant from the nominal pair-track
 777 centers (3200 m for pair 1, 0 m for pair 2, -3200 m for pair 3).
 778

779 5.1.2 Select pairs for the reference-surface calculation

780 **Inputs:**

- 781 *ref_pt*: reference point number for the current fit
 782 *x_atc_ctr*: Along-track coordinate of the reference point
 783 *D_ATL06*: ATL06 data structure
 784 *pair_data*: Structure describing ATL06 pairs, includes mean of strong/weak beam *y_atc* and
 785 *dh_fit_dy*

786 **Outputs:**

787 **validity flags for each segment:**

- 788 *valid_segs.x_slope*: Segments identified as valid based on x-slope consistency
 789 *valid_segs.data*: Segments identified as valid based on ATL06 parameter values.

790 **Validity flags for each pair:**

- 791 *valid_pairs*: Pairs selected for the reference-surface calculation
 792 *valid_pairs.y_slope*: Pairs identified as valid based on y-slope consistency
 793 *y_polyfit_ctr*: y center of the slope regression
 794 *ref_surf/complex_surface_flag*: Flag indicating 0: non-complex surface, 1: complex surface.
 795

796 **Parameters:**

797 *L_search_XT*: The across-track search distance.
 798 *N_search*: Along-track segment search distance
 799 *seg_sigma_threshold_min*: Minimum threshold for accepting errors in segment heights, equal to
 800 0.05 m.

801 **Algorithm:**

802 1. Flag valid segments based on ATL06 values.

803 1a. Count the cycles that contain at least one pair that has *atl06_quality_flag*=0
 804 for both segments. If this number is greater than $N_{cycles}/3$, set
 805 *ref_surf/complex_surface_flag*=0 and set *valid_segs.data* to 1 for segments with
 806 *ATL06_quality_summary* equal to 0. Otherwise, set *ref_surf/complex_surface_flag*=1 and set
 807 *valid_segs.data* to 1 for segments with *snr_significance* < 0.02.

808 1b. Define *seg_sigma_threshold* as the maximum of 0.05 or three times the median of
 809 *sigma_h_li* for segments with *valid_segs.data* equal to 1. Set *valid_segs.data* to 1 for segments
 810 with *h_sigma_li* less than this threshold and *ATL06_quality_summary* equal to 0.

811 1c. Define *valid_pairs.data*: For each pair of segments, set *valid_pairs.data* to 1 when
 812 both segments are marked as valid in *valid_segs.data*.

813 2. Calculate representative values for the *x* and *y* coordinate for each pair, and filter by distance.

814 2a. For each pair containing two defined values, set *pair_data.x* to the segments' *x_atc*
 815 value, and *pair_data.y* to the mean of the segments' *y_atc* values.

816 2b. Calculate *y_polyfit_ctr*, equal to the median of *pair_data.y* for pairs marked valid in
 817 *valid_pairs.data*.

818 2c. Set *valid_pairs.ysearch* to 1 for pairs with $|pair_data.y - y_polyfit_ctr| <$
 819 *L_search_XT*.

820 3. Select pairs based on across-track slope consistency

821 3a. Define *pairs_valid_for_y_fit*, for the across-track slope regression if they are marked
 822 as valid in *valid_pairs.data*, and *valid_pairs.ysearch*, not otherwise.

823 3b. Choose the degree of the regression for across-track slope

824 -If the valid pairs contain at least two different *x_atc* values (separated by at least
 825 18 m), set the along-track degree, *my_regression_y_degree*, to 1, 0 otherwise.

826 -If valid pairs contain at least two different *ref_surf/y_atc* values (separated by at
 827 least 18 m), set the across-track degree, *my_regression_y_degree*, to 1, 0 otherwise.

828 3c. Calculate the formal error in the *y* slope estimates: *y_slope_sigma* is the RSS of the
 829 *h_li_sigma* values for the two beams in the pair divided by the difference in their *y_atc*
 830 values. Based on these, calculate *my_regression_tol*, equal to the maximum of 0.01 or three
 831 times the median of *y_slope_sigma* for valid pairs (*pairs_valid_for_y_fit*).

832 3d. Calculate the regression of *dh_fit_dy* against *pair_data.x* and *pair_data.y* for valid
 833 pairs (*pairs_valid_for_y_fit*). The result is *y_slope_model*, which gives the variation of *dh_fit_dy*
 834 as a function of *x_atc* and *y_atc*. Calculate *y_slope_resid*, the residuals between the *dh_fit_dy*
 835 values and *y_slope_model* for all pairs in *pair_data*.

836 3e. Calculate *y_slope_threshold*, equal to the maximum of *my_regression_tol* and three
 837 times the RDE of *y_slope_resid* for valid pairs.

838 3f. Mark all pairs with $|y_slope_resid| > y_slope_threshold$ as invalid. Re-establish
 839 *pairs_valid_for_y_fit* (based on *valid_pairs.data*, *valid_pairs.y_slope* and *valid_pairs.ysearch*).
 840 Return to step 3d (allow two iterations total).

841 3g. After the second repetition of 3d-f, use the model to mark all pairs with
 842 $|y_slope_resid|$ less than $y_slope_threshold$ with 1 in *valid_pairs.y_slope*, 0 otherwise.

843 4. Select segments based on along-track slope consistency for both segments in the pair

844 4a. Define *pairs_valid_for_x_fit*, valid segments for the along-track slope regression:
 845 segments are valid if they come from pairs marked as valid in *valid_pairs.data* and
 846 *valid_pairs.ysearch*, not otherwise.

847 4b. Choose the degree of the regression for along-track slope

848 -If valid segments contain at least two different *x_atc* values set the along-track
 849 degree, *mx_regression_x_degree*, to 1, 0 otherwise.

850 -If valid segments contain at least two different *y_atc* values, set the across-track
 851 degree, *mx_regression_y_degree*, to 1, 0 otherwise.

852 4c. Calculate along-track slope regression tolerance, *mx_regression_tol*, equal to the
 853 maximum of either 0.01 or three times the median of the *dh_fit_dx_sigma* values for the valid
 854 pairs.

855 4d. Calculate the regression of *dh_fit_dx* against *pair_data.x* and *pair_data.y* for valid
 856 segments (*pairs_valid_for_x_fit*). The result is *x_slope_model*, which gives the variation of
 857 *dh_fit_dx* as a function of *pair_data.x* and *pair_data.y*. Calculate *x_slope_resid*, the residuals
 858 between the *dh_fit_dx* and *x_slope_resid* for all segments for this reference point, *seg_x_center*
 859 and *y_polyfit_ctr*.

860 4e. Calculate *x_slope_threshold*, equal to the maximum of either *mx_regression_tol* or
 861 three times the RDE of *x_slope_resid* for valid segments.

862 4f. Mark *valid_segs.x_slope* with $|x_slope_resid| > x_slope_threshold$ as invalid. Re-
 863 establish *valid_pairs.x_slope* when both *valid_segs.x_slope* equal 1. Re-establish
 864 *pairs_valid_for_x_fit*. Return to step 4d (allow two iterations total).

865 4g. After the second repetition of 4d-f, mark all segments with $|x_slope_resid|$ less than
 866 $x_slope_threshold$ with 1 in *seg_valid_xslope*, 0 otherwise. Define *valid_pairs.x_slope* as 1 for
 867 pairs that contain two segments with *valid_segs.x_slope*=1, 0 otherwise.

868 5. Re-establish *valid_pairs.all*. Set equal to 1 if *valid_pairs.x_slope*, *valid_pairs.y_slope*,
 869 and *valid_pairs.data* are all valid.

870 5a. Identify *unselected_cycle_segs*, as those *D6.cycles* where *valid_pairs.all* are False.
 871

872 5.1.3 Adjust the reference-point y location to include the maximum number of 873 cycles

874 **Inputs:**

875 *D_ATL06*: ATL06 structure for the current reference point.

876 *valid_pairs*: Pairs selected based on parameter values and along- and across-track slopes.

877 **Outputs:**

878 *ref_surf/y_atc*: Adjusted fit-point center *y*.

879 *valid_pairs*: validity masks for pairs, updated to include those identified as valid based on the
 880 spatial search around *y_atc_ctr*.

881 **Parameters:**

882 *L_search_XT*: Across-track search length (equal to 110 m)

883 **Algorithm:**

884 1. Define *y0* as the median of the unique integer values of the pair center *y_atc* for all
885 valid pairs. Set a range of *y* values, *y0_shifts*, as $\text{round}(y0) \pm 100$ meters in 2-meter increments.

886 2. For each value of *y0_shifts* (*y0_shift*), set a counter, *selected_seg_cycle_count*, to the
887 number of distinct cycles for which both segments of the pair are contained entirely within the *y*
888 interval [*y0_shift* - *L_search_XT*, *y0_shift* + *L_search_XT*]. Add to this, the number of distinct
889 cycles represented by unpaired segments contained within that interval, weighted by 0.01. The
890 sum is called *score*.

891 3. Search for an optimal *y*-center value (with the most distinct cycles). Set *y_best* to the
892 value of *y0_shift* that maximizes *score*. If there are multiple *y0_shift* values with the same,
893 maximum *score*, set to the median of the *y0_shift* values with the maximum *score*.

894 4. Update *valid_pairs* to include all pairs with *y_atc* within $\pm L_search_XT$ from
895 *y_atc_ctr*.

896 **5.1.4 Calculate the reference surface and corrected heights for selected pairs**

897 **Inputs:**

898 *D_ATL06*: ATL06 structure for the current reference point, containing parameters for each
899 segment:

900 *x_atc*: along-track coordinate

901 *y_atc*: across-track coordinate

902 *delta_t*: time for the segment

903 *pair_data*: Structure containing information about ATL06 pairs. Must include:

904 *y_atc*: Pair-center across-track coordinates

905 *valid_pairs*: Pairs selected based on parameter values and along- and across-track slope.

906 *x_atc_ctr*: The reference point along-track x coordinate (equal to *ref_surf/x_atc*).

907 *y_atc_ctr*: The reference point across-track y coordinate (equal to *ref_surf/y_atc*)

908 **Outputs:**

909 *ref_surf/deg_x*: Degree of the reference-surface polynomial in the along-track direction

910 *ref_surf/deg_y*: Degree of the reference-surface polynomial in the across-track direction

911 *ref_surf/poly_coeffs*: Polynomial coefficients of the reference-surface fit

912 *ref_surf/poly_coeffs_sigma*: Formal error in polynomial coefficients of the reference-surface fit

913 *ref_surf/slope_change_rate_x*: Rate of change of the x component of the surface slope

914 *ref_surf/slope_change_rate_x_sigma*: Formal error in the rate of change of the x component of
915 the surface slope

916 *ref_surf/slope_change_rate_y*: Rate of change of the y component of the surface slope

917 *ref_surf/slope_change_rate_y_sigma*: Formal error in the rate of change of the y component of
918 the surface slope

919 *r_seg*: Segment residuals from the reference-surface model

920 */ptx/h_corr*: Partially filled-in per-cycle corrected height for cycles used in reference surface

921 */ptx/h_corr_sigma*: Partially filled-in per-cycle formal error in corrected height for cycles used in
922 reference surface

923 *ref_surf_cycles*: A list of cycles used in defining the reference surface

924 *C_m_surf*: Covariance matrix for the reference-polynomial and surface-change model

925 *fit_columns_surf*: Mask identifying which components of the combined reference-polynomial
 926 and surface-change model were included in the fit.

927 *poly_exponent_x*: The x degrees corresponding to the columns of matrix used in fitting the
 928 reference surface to the data

929 *poly_exponent_y*: The y degrees corresponding to the columns of matrix used in fitting the
 930 reference surface to the data

931 *selected_segments*: A set of flags indicating which segments were selected by the iterative
 932 fitting process.

933 Partially filled-n per-cycle ATL11 output variables (see table 4-3) for cycles used in reference
 934 surface

935 **Parameters:**

936 *poly_max_degree_AT*: Maximum polynomial degree for the along-track fit, equal to 3.

937 *poly_max_degree_XT*: Maximum polynomial degree for the across-track fit, equal to 2.

938 *slope_change_t0*: Half the duration of the mission (equal to the time of the last-possible
 939 elevation value minus the time of the start of data collection, divided by two).

940 *max_fit_iterations*: Maximum number of iterations for surface fitting, with acceptable residuals,
 941 equal to 20.

942 *xy_scale*: The horizontal scaling value used in polynomial fits, equal to 100 m

943 *t_scale*: The time scale used in polynomial fits, equal to seconds in 1 year.

944 **Algorithm:**

945 1. Build the cycle design matrix: **G_{zp}** is a matrix that has one column for each distinct
 946 cycle in *selected_pairs* and one row for each segment whose pair is in *selected_pairs*. For each
 947 segment, the corresponding row of **G_{zp}** is 1 for the column matching the cycle for that segment
 948 and zero otherwise.

949 2. Select the polynomial degree.

950 The degree of the x polynomial, *ref_surf/deg_x*, is:

951 $\min(\text{poly_max_degree_AT}, \text{maximum}(\text{number of distinct values of } \text{round}((x_atc - x_atc_ctr)/20)$
 952 among the selected segments in any one cycle) - 1), and the degree of the y polynomial,

953 *ref_surf/deg_y*, is : $\min(\text{poly_max_degree_XT}, \text{number of distinct values of}$
 954 $\text{round}((\text{pair_data.y_atc} - \text{y_atc_ctr})/20)$ among the selected pairs)

955 3. Perform an iterative fit for the reference-surface polynomial.

956 3a. Define *degree_list_x* and *degree_list_y*: This array defines the x and y degree of the
 957 polynomial coefficients in the polynomial surface model. There is one component for each
 958 unique degree combination of x degrees between 0 and *ref_surf/deg_x* and for y degree between
 959 0 and *ref_surf/deg_y* such that $x_degree + y_degree \leq \max(\text{ref_surf/deg_x}, \text{ref_surf/deg_y})$,
 960 except that there is no $x_degree=0$ and $y_degree=0$ combination. They are sorted first by the
 961 sum of the x and y degrees, then by x degree, then by y degree.

962 3b. Define the polynomial fit matrix. **S_{fit_poly}** has one column for each element of
 963 the polynomial degree arrays, with values equal to $((x_atc - x_atc_ctr)/xy_scale)^{x_degree} ((y_atc -$
 964 $y_atc_ctr)/xy_scale)^{y_degree}$. There is one row in the matrix for every segment marked as *selected*.

965 3c. If the time span is longer than 1.5 years, define slope-change matrices,

966 **S_{fit_slope_change}**. The first column of the matrix gives the rate of slope change in the x
 967 component, equal to $(x_atc - x_atc_ctr)/xy_scale * (\text{delta_time} - \text{slope_change_t0})/t_scale$. The
 968 second column gives the rate of slope change in the y component, equal to $(y_atc -$
 969 $y_atc_ctr)/xy_scale * (\text{delta_time} - \text{slope_change_t0})/t_scale$.

970 3d. Build the surface matrix, **G_surf**, and the combined surface and cycle-height matrix,
 971 **G_surf_zp**: The surface matrix is equal to the horizontal catenation of **S_fit_poly**, and, if
 972 defined, **S_fit_slope_change**. The combined surface and cycle-height matrix, **G_surf_zp**, is
 973 equal to the horizontal catenation of **G_surf** and **G_zp**.

974 3e. Subset the fitting matrix. Subset **G_surf_zp** by row to include only rows
 975 corresponding to selected segments to produce **G** (on the first iteration, all are *selected*). Next,
 976 subset **G** by column, first to eliminate all-zero columns, and second to include only columns that
 977 are linearly independent from one another: calculate the normalized correlation between each
 978 pair of columns in **G**, and if the correlation is equal to unity, eliminate the column with the
 979 higher weighted degree ($poly_wt_sum = x_degree + 1.1*y_degree$, with the factor of 1.1
 980 chosen to avoid ties). Identify the selected columns in the matrix as *fit_columns*. If more than
 981 three of the original surface-change columns have been eliminated, set the
 982 *ref_surf/complex_surface_flag* to *True*, mark all columns corresponding to polynomial
 983 coefficients of combined x and y degree greater than 1 as *False* in *fit_columns*.

984 3f. Check whether the inverse problem is under- or even-determined: If the number of
 985 *selected_segments* is less than the number of columns of **G**, eliminate remaining columns of **G** in
 986 descending order of *poly_wt_sum* until the number of columns of **G** is less than the number of
 987 *selected_segments*.

988 3g. Generate the data-covariance matrix, **C_d**. The data-covariance matrix is a square
 989 matrix whose diagonal elements are the squares of the *h_li_sigma* values for the selected
 990 segments.

991 3h. Calculate the polynomial fit. Initialize **m_surf_zp**, the reference model, to a vector of
 992 zero values, with one value for each column of **G_surf_zp**. Calculate the generalized inverse
 993 (equation 7), of **G**, **G_g**. If the inversion calculation returns an error, or if any row of **G_g** is all-
 994 zero (indicating some parameters are not linearly independent), report fit failure and return.
 995 Otherwise, multiply **G_g** by the subset of *h_li* corresponding to the selected segment to give **m**,
 996 containing values for the parameters selected in *fit_columns*. Fill in the components of
 997 **m_surf_zp** flagged in *fit_columns* with the values in **m**.

998 3i. Calculate model residuals for all segments, *r_seg*, equal to $h_li - G_surf_dz * m_surf_zp$.
 999 The subset of *r_seg* corresponding to *selected* segments is *r_fit*.

1000 3j. Calculate the fitting tolerance, *r_tol*, equal to three times the RDE of the
 1001 r_fit/h_li_sigma for all *selected* segments. Calculate the reduced chi-squared value for these
 1002 residuals, *ref_surf/misfit_chi2*, equal to $r_fit^T C_d^{-1} r_fit$. Calculate the *P* value for the misfit,
 1003 equal to one minus the CDF of a chi-squared distribution with *m-n* degrees of freedom for
 1004 *ref_surf/misfit_chi2*, where *m* is the number of rows in **G**, and *n* is the number of columns.

1005 3k. If the *P* value is less than 0.025 and fewer than *max_fit_iterations* have taken place,
 1006 mark all segments for which $|r_seg/h_li_sigma| < r_tol$ as *selected*, and return to 3e. Otherwise,
 1007 continue to 3k.

1008 3l. Propagate the errors. Based on the most recent value of **C_d**, generate a revised data-
 1009 covariance matrix, **C_dp**, whose diagonals values are the maximum of $h_li_sigma^2$ and
 1010 $RDE(r_fit)^2$. Calculate the model covariance matrix, **C_m** using equation 9. If any of the
 1011 diagonal elements of **C_m** are larger than 10^4 , report a fit failure and return. Fill in elements of
 1012 **m_surf_zp** that are marked as valid in *fit_columns* with the square roots of the corresponding
 1013 diagonal elements of **C_m**. If any of the errors in the polynomial coefficients are larger than 10,
 1014 set *ref_surf/fit_quality*=1.

1015 4. Return a list of cycles used in determining the reference surface in *ref_surf_cycles*. These
 1016 cycles have columns in **G** that contain a valid pair, and for which the steps 3e and 3j did not
 1017 eliminate the degree of freedom. For these cycles, partially fill in the values of */ptx/h_corr* and
 1018 */ptx/h_corr_sigma*, from **m** and **m_sigma**. Similarly, fill in values for
 1019 */ptx/h_corr_sigma_systematic* (Equation 12) and */ptx/delta_time*, as well as all variables in Table
 1020 4-3. Set */ptx/h_corr*, */ptx/h_corr_sigma*, */ptx/h_corr_sigma_systematic* to *NaN* for those cycles
 1021 that have uncorrelated error estimates greater than 15 m.
 1022 Values from Table 4-2 defining the fitted reference surface are also reported including
 1023 *ref_surf/poly_coeffs*, and *ref_surf/poly_coeffs_sigma*, *ref_surf/slope_change_rate_x*,
 1024 *ref_surf/slope_change_rate_y*, *ref_surf/slope_change_rate_x_sigma*, and
 1025 *ref_surf/slope_change_rate_y_sigma*.
 1026 Return **C_m_surf**, the portion of **C_m** corresponding to the polynomial and slope-change
 1027 components of **C_m**. Return *selected_cols_surf*, the subset of *selected_cols* corresponding to the
 1028 surface polynomial and slope-change parameters.
 1029 Return the reduced chi-square value for the last iteration, *ref_surf/misfit_chi2r*, equal to
 1030 *ref_surf/misfit_chi2/(m-n)*.
 1031

1032 5.1.5 Calculate corrected heights for cycles with no selected pairs.

1033 **Inputs:**

1034 **C_m_surf**: Covariance matrix for the reference-surface model.
 1035 *degree_list_x*, *degree_list_y*: List of x-, y-, degrees for which the reference-surface calculation
 1036 attempted an estimate.
 1037 *selected_cols_surf*: Parameters of the combined reference-surface and slope-change model for
 1038 which the inversion returned a value. There should be one value for each row/column of
 1039 **C_m_surf**.
 1040 *x_atc_ctr*, *y_atc_ctr*: Center point for the surface fit (equal to *ref_surf/x_atc*, *ref_surf/y_atc*)
 1041 *selected_segments*: Boolean array indicating segments selected for the reference-surface
 1042 calculation
 1043 *valid_segs.x_slope*: Segments identified as valid based on x-slope consistency
 1044 *valid_segs.data*: Segments identified as valid based on ATL06 parameter values.
 1045 *pair_number*: Pair number for each segment
 1046 *h_li*: Land-ice height for each segment
 1047 *h_li_sigma*: Formal error in *h_li*.
 1048 */ptx/h_corr*: Partially filled-in per-cycle corrected height
 1049 */ptx/h_corr_sigma*: Partially filled-in per-cycle corrected height error
 1050 *ref_surf/poly_coeffs*: Polynomial coefficients from 2-d reference-surface fit
 1051 *ref_surf_cycles*: A list of cycles used in defining the reference surface
 1052 *ref_surf/slope_change_rate_x*, *ref_surf/slope_change_rate_y*: Rate of change of the x and y
 1053 components of the surface slope
 1054 *ref_surf/N_slope*, *ref_surf/E_slope*: slope components of reference surface
 1055 *sigma_geo_r*: Radial component of the geolocation error for the crossing track
 1056 *D_ATL06*: ATL06 data structure
 1057 Partially filled-in per-cycle ATL11 output variables (see table 4-3)

1058 **Outputs:**

1059 */ptx/h_corr*: Per-cycle corrected height
 1060 */ptx/h_corr_sigma*: Per-cycle corrected height error
 1061 *selected_segments*: A set of arrays listing the selected segments for each cycle.
 1062 Per-cycle ATL11 output variables (see table 4-3).

1063 **Algorithm:**

1064 1. Identify the segments marked as valid in *valid_segs.data* and *valid_segs.x_slope* that are not
 1065 members of the cycles in *ref_surf_cycles*. Label these as *non_ref_segments*.
 1066 2. Build **G_other**, a polynomial-fitting matrix for the *non_ref_segments*. **G_other** will include
 1067 only the polynomial components listed in *degree_list_x* and *degree_list_y*, and (if the mission
 1068 has been going on for at least 1.5 years) the slope-change components. Multiply **G_other** by
 1069 [*ref_surf/poly_coeffs*, *ref_surf/slope_change_rate_x*, *ref_surf/slope_change_rate_y*] to give
 1070 corrected heights, *z_kc*.
 1071 3. Take the subset of **G_other** corresponding to the components in *fit_cols_surf* to make
 1072 **G_other_surf**. Propagate the polynomial surface errors and surface-height errors for
 1073 *non_ref_segments* based on **G_other_surf**, **C_m_surf**, and *h_li_sigma* using equation
 1074 11. These errors are *z_kc_sigma*.
 1075 4. Identify the segments in *non_ref_segments* for each cycle, and, from among these, select the
 1076 one with the smallest *z_kc_sigma*. If, for this cycle, *z_kc_sigma* is less than 15 m, fill in the
 1077 corresponding values of */ptx/h_corr* and */ptx/h_corr_sigma*. For cycles containing no valid
 1078 segments, report invalid data as NaN. Similarly, fill in the variables in Table 4-3, with the value
 1079 from the segment with the smallest *z_kc_sigma*.
 1080

1081 **5.1.6 Calculate corrected heights for crossover data points**

1082 **Inputs:**

1083 *C_m_surf*: Covariance matrix for the reference surface model.
 1084 *C_m_surf*: Covariance matrix for the reference-surface model.
 1085 *x_atc_ctr*, *y_atc_ctr*: Center point for the surface fit, in along-track coordinates
 1086 *lat_d*, *lon_d*: Latitude and longitude for the adjusted datum reference point (from */ptx/latitude*,
 1087 */ptx/longitude*)
 1088 *PT*: Pair track for the surface fit
 1089 *RGT*: RGT for the surface fit
 1090 *ref_surf/rgt_azimuth*: The azimuth of the RGT, relative to local north
 1091 *lat_c*, *lon_c*: Location for crossover data
 1092 *time_c*: Time for crossover data
 1093 *h_c*: Elevations for crossover data
 1094 *sigma_h_c*: Estimated errors for crossover data

1095 **Outputs:**

1096 *ref_pt*: reference point (for the reference track)
 1097 *pt*: pair track for the crossing-track points
 1098 *crossing_track_data/rgt*: Reference ground track for the crossing-track point
 1099 *crossing_track_data/delta_time*: time for the crossing-track point
 1100 *crossing_track_data/h_corr*: corrected elevation for the crossing-track points
 1101 *crossing_track_data/h_corr_sigma*: error in the corrected elevation for the crossing_track points

1102 *crossing_track_data/h_corr_sigma_systematic*: Error component in the corrected elevation due
 1103 to pointing and orbital errors.

1104 *crossing_track_data/along_track_rss*:

1105 **Parameters:**

1106 *L_search_XT*: Across-track search distance

1107 **Algorithm (executed independently for the data from each cycle of the mission):**

1108 1. Project data points into the along-track coordinate system:

1109 1a: Calculate along-track and across-track vectors:

1110 $x_hat = [\cos(\text{ref_surf}/\text{rgt_azimuth}), \sin(\text{ref_surf}/\text{rgt_azimuth})]$

1111 $y_hat = [\sin(\text{ref_surf}/\text{rgt_azimuth}), -\cos(\text{ref_surf}/\text{rgt_azimuth})]$

1112 1b. Calculate the R_earth , the WGS84 radius at lat_d .

1113 1c: Project the crossover data points into a local projection centered on the fit

1114 center:

1115 $N_d = R_earth (\text{lat}_c - \text{lat}_d)$

1116 $E_d = R_earth \cos(\text{lat}_d) (\text{lon}_c - \text{lon}_d)$

1117 1d: Calculate the x and y coordinates for the data points, relative to the fit-center point:

1118 $dx_c = \langle x_hat, [E_c, N_c] \rangle$

1119 $dy_c = \langle y_hat, [E_c, N_c] \rangle$

1120 Here $\langle \mathbf{a}, \mathbf{b} \rangle$ is the inner (dot) product of \mathbf{a} and \mathbf{b} .

1121 2. Calculate the fitting matrix using equation 6.

1122 3. Calculate the errors at each point using the fitting matrix and C_m , using on equation 11.

1123 4. Select the minimum-error data point and report the values in Table 4-1.

1124 5. Calculate the systematic error in the corrected height:

1125 $\text{crossing_track_data}/h_sigma_sigma_systematic = (\text{sigma_geo_r}^2 + (N_d$
 1126 $\text{ref_surf}/n_slope)^2 + ((E_d \text{ref_surf}/e_slope)^2)^{1/2}$

1127 6. Calculate the along-track RSS for the selected segment. For each selected crossing segment
 1128 calculate the endpoint heights (equal to the segment center height plus or minus 20 meters times
 1129 the segment's along-track slope), and calculate the RSS of the differences between these heights
 1130 and the center heights of the previous and subsequent segments. If this RSS difference is greater
 1131 than 10 m for any cycle, do not report any parameters for that segment's cycle.

1132 5.1.7 Provide error-averaged values for selected ATL06 parameters

1133 **Inputs:**

1134 *ATL06 data structure*: ATL06 data to be averaged

1135 *Selected_segments*: A set of arrays listing the selected segments for each cycle.

1136 *Parameter_list*: A list of parameters to be averaged

1137 **Outputs:**

1138 *Parameter_averages*: One value for each parameter and each cycle

1139 **Algorithm:**

1140 1. For each cycle, select the values of h_li_sigma based on the values within *selected_segments*.

1141 Calculate a set of weights, w_i , such that the sum of the weights is equal to 1 and each weight is

1142 proportional to the inverse square of h_li_sigma . If only one value is present in

1143 *selected_segments*, $w_1=1$.

1144 2. For each parameter, multiply the weights for each cycle by the parameter values, report the
 1145 averaged value in *parameter_averages*.

1146 **5.1.8 Provide miscellaneous ATL06 parameters**

1147 **Inputs:**

1148 *ATL06 data structure*: ATL06 data to be averaged

1149 *Selected_segments*: A set of arrays listing the selected segments for each cycle.

1150 **Outputs:**

1151 Weighted-averaged parameter values, with one value per cycle, filled in with NaN for cycles
 1152 with no selected segments

1153 *cycle_stats/h_robust_sprd*

1154 *cycle_stats/h_li_rms_mean*

1155 *cycle_stats/r_eff*

1156 *cycle_stats/tide_ocean*

1157 *cycle_stats/dac*

1158 *cycle_stats/bsnow_h*

1159 *cycle_stats/x_atc*

1160 *cycle_stats/y_atc*

1161 *cycle_stats/sigma_geo_h*

1162 *cycle_stats/sigma_geo_at*

1163 *cycle_stats/sigma_geo_xt*

1164 *cycle_stats/h_mean*

1165 *ref_surf/dem_h*

1166 *ref_surf/geoid_h*

1167 Parameter minimum values, with one value per cycle, filled in NaN for cycles with no selected
 1168 segments:

1169 *cycle_stats/cloud_flg_asr*

1170 *cycle_stats/cloud_flg_atm*

1171 *cycle_stats/bsnow_conf*

1172 Other parameters:

1173 *cycle_stats/strong_spot*: The laser beam number for the strong beam in the pair

1174 **Algorithm:**

1175 1. Select the segments for the cycle indicated in *selected_segments* from the

1176 *ATL06_data_structure*.

1177 2: Based on *h_li_sigma*, calculate the segment weights using equation 14.

1178 3.1 For ATL06 parameters *h_robust_sprd*, *h_li_rms*, *r_eff*, *tide_ocean*, *dac*, *bsnow_h*, *x_atc*,

1179 *y_atc*, *sigma_geo_h*, *sigma_geo_at*, *sigma_geo_xt*, and *h_mean* calculate the weighted average

1180 of the parameter based on the segment weights. The output parameter names are the same as the

1181 input parameter names, in the *cycle_stats* group.

1182 3.2 For ATL06 parameters *dem_h* and *geoid_h*, by regression between the measurement

1183 location and the reference point location. The output parameter names are the same as the input

1184 parameter names, in the *ref_surf* group.

1185 4. For ATL06 parameters *cloud_flg_asr* and *cloud_flg_atm* report the best (minimum) value

1186 from among the selected values. For *bsnow_conf* report the maximum value from among the

1187 selected values.

1188 5. For the *cycle_stats/strong_spot* attribute, report the laser beam number for the strong beam in
 1189 the pair.
 1190

1191 **5.1.9 Characterize the reference surface**

1192 **Inputs:**

1193 *poly_coefs*: Coefficients of the surface polynomial

1194 *poly_coeff_sigma*: Error estimates for the surface polynomial

1195 *degree_list_x, degree_list_y*: exponents of the reference-surface polynomial for which the
 1196 reference-surface fit returned a coefficient

1197 *rgt_azimuth*: the azimuth of the reference ground track

1198 **Parameters:**

1199 *poly_max_degree_AT, poly_max_degree_XT*: Maximum polynomial degree allowed in x and y.

1200 **Outputs:**

1201 *ref_surf/n_slope*: the north component of the reference-surface slope

1202 *ref_surf/e_slope*: the east component of the reference-surface slope

1203 *ref_surf/at_slope*: the along-track component of the reference-surface slope

1204 *ref_surf/xt_slope*: the across-track component of the reference-surface slope

1205 *ref_surf/rms_slope_fit*: the rms slope of the reference surface

1206 *ref_surf/poly_ref_surf*: the polynomial reference surface coefficients

1207 *ref_surf/poly_ref_surf_sigma*: error estimates for *ref_surf/poly_ref_surf*

1208 **Procedure:**

1209 1. Calculate the coordinates of a grid of northing and easting offsets around the reference points,
 1210 each between -50 m and 50 m in 10-meter increments: dN, dE

1211 2. Translate the coordinates into along and across-track coordinates:

1212 $dx = \cos(\text{rgt_azimuth}) * dN + \sin(\text{rgt_azimuth}) * dE$

1213 $dy = \sin(\text{rgt_azimuth}) * dN - \cos(\text{rgt_azimuth}) * dE$

- 1214 3. Calculate the polynomial surface elevations for the grid points by evaluating the polynomial
1215 surface at dx and dy : z_poly
- 1216 4. Fit a plane to z_poly as a function of dN and dE . The North coefficient of the plane is
1217 ref_surf/n_slope , the east component is ref_surf/e_slope , the RMS misfit of the plane is
1218 ref_surf/rms_slope_fit . If either component of the slope has a magnitude larger than 0.2, add 2 to
1219 $ref_surf/fit_quality$.
- 1220 5. Fit a plane to z_poly as a function of dx and dy . The along-track coefficient of the plane is
1221 ref_surf/at_slope , the across-track component is ref_surf/xt_slope .
- 1222 6. Generate the polynomial exponents for the output columns. The list of components for
1223 the output variables has one component for each unique degree combination of x degrees
1224 between 0 and ref_surf/deg_x and for y degree between 0 and ref_surf/deg_y such that x_degree
1225 $+ y_degree \leq \max(poly_max_degree_XT, poly_max_degree_AT)$, except that there is no
1226 $x_degree=0$ and $y_degree=0$ combination. They are sorted first by the sum of the x and y
1227 degrees, then by x degree, then by y degree.
1228 Match the polynomial degrees for this reference point's coefficients to these degrees, and write
1229 each value of $poly_ref_surf$ and $poly_ref_surf_sigma$ into the appropriate position of the output
1230 array, filling missing values with *invalid*.
- 1231

1232 **6.0 APPENDIX A: GLOSSARY**

1233 This appendix defines terms that are used in ATLAS ATBDs, as derived from a document
 1234 circulated to the SDT, written by Tom Neumann. Some naming conventions are borrowed from
 1235 **Spots, Channels and Redundancy Assignments** (ICESat-2-ATSYS-TN-0910) by P. Luers.
 1236 Some conventions are different than those used by the ATLAS team for the purposes of making
 1237 the data processing and interpretation simpler.

1238
 1239 **Spots.** The ATLAS instrument creates six spots on the ground, three that are weak and three that
 1240 are strong, where strong is defined as approximately four times brighter than weak. These
 1241 designations apply to both the laser-illuminated spots and the instrument fields of view. The
 1242 spots are numbered as shown in Figure 1. At times, the weak spots are leading (when the
 1243 direction of travel is in the ATLAS +x direction) and at times the strong spots are leading.
 1244 However, the spot number does not change based on the orientation of ATLAS. The spots are
 1245 always numbered with 1L on the far left and 3R on the far right of the pattern. Not: beams,
 1246 footprints.

1247
 1248 **Laser pulse (pulse for short).** Individual pulses of light emitted from the ATLAS laser are
 1249 called laser pulses. As the pulse passes through the ATLAS transmit optics, this single pulse is
 1250 split into 6 individual transmit pulses by the diffractive optical element. The 6 pulses travel to
 1251 the earth’s surface (assuming ATLAS is pointed to the earth’s surface). Some attributes of a laser
 1252 pulse are the wavelength, pulse shape and duration. Not: transmit pulse, laser shot, laser fire.

1253
 1254 **Laser Beam.** The sequential laser pulses emitted from the ATLAS instrument that illuminate
 1255 spots on the earth’s surface are called laser beams. ATLAS generates 6 laser beams. The laser
 1256 beam numbering convention follows the ATLAS instrument convention with strong beams
 1257 numbered 1, 3, and 5 and weak beams numbered 2, 4, and 6 as shown in the figures. Not:
 1258 beamlet.

1259
 1260 **Transmit Pulse.** Individual pulses of light emitted from the ICESat-2 observatory are called
 1261 transmit pulses. The ATLAS instrument generates 6 transmit pulses of light from a single laser
 1262 pulse. The transmit pulses generate 6 spots where the laser light illuminates the surface of the
 1263 earth. Some attributes of a given transmit pulse are the wavelength, the shape, and the energy.
 1264 Some attributes of the 6 transmit pulses may be different. Not: laser fire, shot, laser shot, laser
 1265 pulse.

1266
 1267 **Reflected Pulse.** Individual transmit pulses reflected off the surface of the earth and viewed by
 1268 the ATLAS telescope are called reflected pulses. For a given transmit pulse, there may or may
 1269 not be a reflected pulse. Not: received pulse, returned pulse.

1270
 1271 **Photon Event.** Some of the energy in a reflected pulse passes through the ATLAS receiver
 1272 optics and electronics. ATLAS detects and time tags some fraction of the photons that make up
 1273 the reflected pulse, as well as background photons due to sunlight or instrument noise. Any
 1274 photon that is time tagged by the ATLAS instrument is called a photon event, regardless of
 1275 source. Not: received photon, detected photon.

1276

1277 **Reference Ground Track (RGT).** The reference ground track (RGT) is the track on the earth at
1278 which a specified unit vector within the observatory is pointed. Under nominal operating
1279 conditions, there will be no data collected along the RGT, as the RGT is spanned by GT2L and
1280 GT2R (which are not shown in the figures, but are similar to the GTs that are shown). During
1281 spacecraft slews or off pointing, it is possible that ground tracks may intersect the RGT. The
1282 precise unit vector has not yet been defined. The ICESat-2 mission has 1387 RGTs, numbered
1283 from 0001xx to 1387xx. The last two digits refer to the cycle number. Not: ground tracks, paths,
1284 sub-satellite track.

1285
1286 **Cycle Number.** Over 91 days, each of the 1387 RGTs will be targeted in the Polar Regions
1287 once. In subsequent 91-day periods, these RGTs will be targeted again. The cycle number
1288 tracks the number of 91-day periods that have elapsed since the ICESat-2 observatory entered the
1289 science orbit. The first 91-day cycle is numbered 01; the second 91-day cycle is 02, and so on.
1290 At the end of the first 3 years of operations, we expect the cycle number to be 12. The cycle
1291 number will be carried in the mid-latitudes, though the same RGTs will (in general) not be
1292 targeted more than once.

1293
1294 **Sub-satellite Track (SST).** The sub-satellite track (SST) is the time-ordered series of latitude
1295 and longitude points at the geodetic nadir of the ICESat-2 observatory. In order to protect the
1296 ATLAS detectors from damage due to specular returns, and the natural variation of the position
1297 of the observatory with respect to the RGT throughout the orbit, the SST is generally not the
1298 same as the RGT. Not: reference ground track, ground track.

1299
1300 **Ground Tracks (GT).** As ICESat-2 orbits the earths, sequential transmit pulses illuminate six
1301 ground tracks on the surface of the earth. The track width is approximately 10m wide. Each
1302 ground track is numbered, according to the laser spot number that generates a given ground
1303 track. Ground tracks are therefore always numbered with 1L on the far left of the spot pattern
1304 and 3R on the far right of the spot pattern. Not: tracks, paths, reference ground tracks, footpaths.

1305
1306 **Reference Pair Track (RPT).** The reference pair track is the imaginary line halfway between
1307 the planned locations of the strong and weak ground tracks that make up a pair. There are three
1308 RPTs: RPT1 is spanned by GT1L and GT1R, RPT2 is spanned by GT2L and GT2R (and may be
1309 coincident with the RGT at times), and RPT3 is spanned by GT3L and GT3R. Note that this is
1310 the planned location of the midway point between GTs. We will not know this location very
1311 precisely prior to launch. Not: tracks, paths, reference ground tracks, footpaths, pair tracks.

1312
1313 **Pair Track (PT).** The pair track is the imaginary line half way between the actual locations of
1314 the strong and weak ground tracks that make up a pair. There are three PTs: PT1 is spanned by
1315 GT1L and GT1R, PT2 is spanned by GT2L and GT2R (and may be coincident with the RGT at
1316 times), and PT3 is spanned by GT3L and GT3R. Note that this is the actual location of the
1317 midway point between GTs, and will be defined by the actual location of the GTs. Not: tracks,
1318 paths, reference ground tracks, footpaths, reference pair tracks.

1319
1320 **Pairs.** When considered together, individual strong and weak ground tracks form a pair. For
1321 example, GT2L and GT2R form the central pair of the array. The pairs are numbered 1 through

1322 3: Pair 1 is comprised of GT1L and GT1R, pair 2 is comprised of GT2L and GT2R, and pair 3 is
1323 comprised of GT3L and 3R.

1324
1325 **Along-track.** The direction of travel of the ICESat-2 observatory in the orbit frame is defined as
1326 the along-track coordinate, and is denoted as the +x direction. The positive x direction is
1327 therefore along the Earth-Centered Earth-Fixed velocity vector of the observatory. Each pair has
1328 a unique coordinate system, with the +x direction aligned with the Reference Pair Tracks.

1329
1330 **Across-track.** The across-track coordinate is y and is positive to the left, with the origins at the
1331 Reference Pair Tracks.

1332
1333 **Segment.** An along-track span (or aggregation) of PE data from a single ground track or other
1334 defined track is called a segment. A segment can be measured as a time duration (e.g. from the
1335 time of the first PE to the time of the last PE), as a distance (e.g. the distance between the
1336 location of the first and last PEs), or as an accumulation of a desired number of photons.
1337 Segments can be as short or as long as desired.

1338
1339 **Signal Photon.** Any photon event that an algorithm determines to be part of the reflected pulse.

1340
1341 **Background Photon.** Any photon event that is not classified as a signal photon is classified as a
1342 background photon. Background photons could be due to noise in the ATLAS instrument (e.g.
1343 stray light, or detector dark counts), sunlight, or mis-classified signal photons. Not: noise
1344 photon.

1345
1346 **h_**.** Signal photons will be used by higher-level products to determine height above the
1347 WGS-84 reference ellipsoid, using a semi-major axis (equatorial radius) of 6378137m and a
1348 flattening of 1/298.257223563. This can be abbreviated as ‘ellipsoidal height’ or ‘height above
1349 ellipsoid’. These heights are denoted by h; the subscript ** will refer to the specific algorithm
1350 used to determine that elevation (e.g. is = ice sheet algorithm, si = sea ice algorithm, etc...). Not:
1351 elevation.

1352
1353 **Photon Cloud.** The collection of all telemetered photon time tags in a given segment is the (or
1354 a) photon cloud. Not: point cloud.

1355
1356 **Background Count Rate.** The number of background photons in a given time span is the
1357 background count rate. Therefore a value of the background count rate requires a segment of PEs
1358 and an algorithm to distinguish signal and background photons. Not: Noise rate, background
1359 rate.

1360
1361 **Noise Count Rate.** The rate at which the ATLAS instrument receives photons in the absence of
1362 any light entering the ATLAS telescope or receiver optics. The noise count rate includes PEs
1363 due to detector dark counts or stray light from within the instrument. Not: noise rate,
1364 background rate, and background count rate.

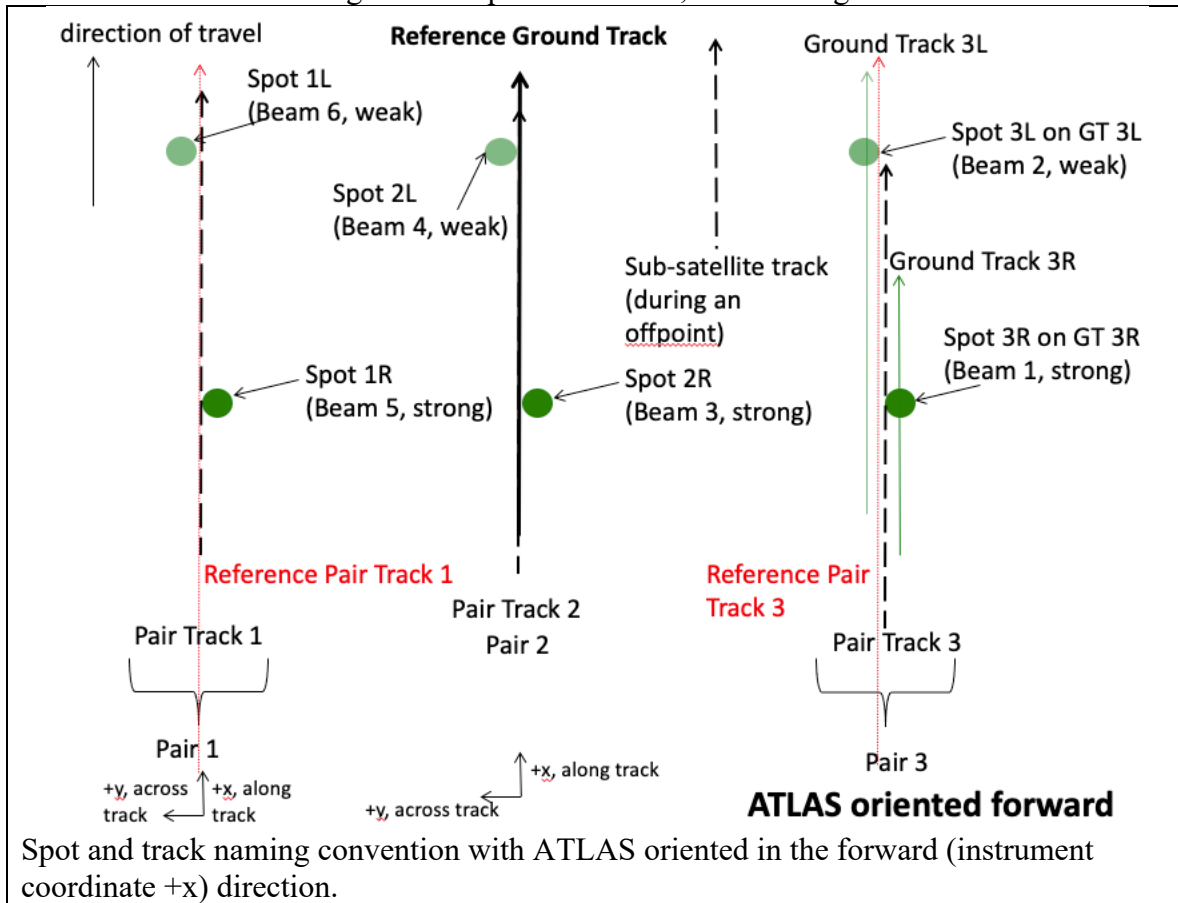
1365

1366 **Telemetry band.** The subset of PEs selected by the science algorithm on board ATLAS to be
 1367 telemetered to the ground is called the telemetry band. The width of the telemetry band is a
 1368 function of the signal to noise ratio of the data (calculated by the science algorithm onboard
 1369 ATLAS), the location on the earth (e.g. ocean, land, sea ice, etc...), and the roughness of the
 1370 terrain, among other parameters. The widths of telemetry bands are adjustable on-orbit. The
 1371 telemetry bandwidth is described in Section 7 or the ATLAS Flight Science Receiver Algorithms
 1372 document. The total volume of telemetered photon events must meet the data volume constraint
 1373 (currently 577 GBits/day).

1374
 1375 **Window, Window Width, Window Duration.** A subset of the telemetry band of PEs is called a
 1376 window. If the vertical extent of a window is defined in terms of distance, the window is said to
 1377 have a width. If the vertical extent of a window is defined in terms of time, the window is said to
 1378 have a duration. The window width is always less than or equal to the telemetry band.

1379
 1380
 1381
 1382
 1383

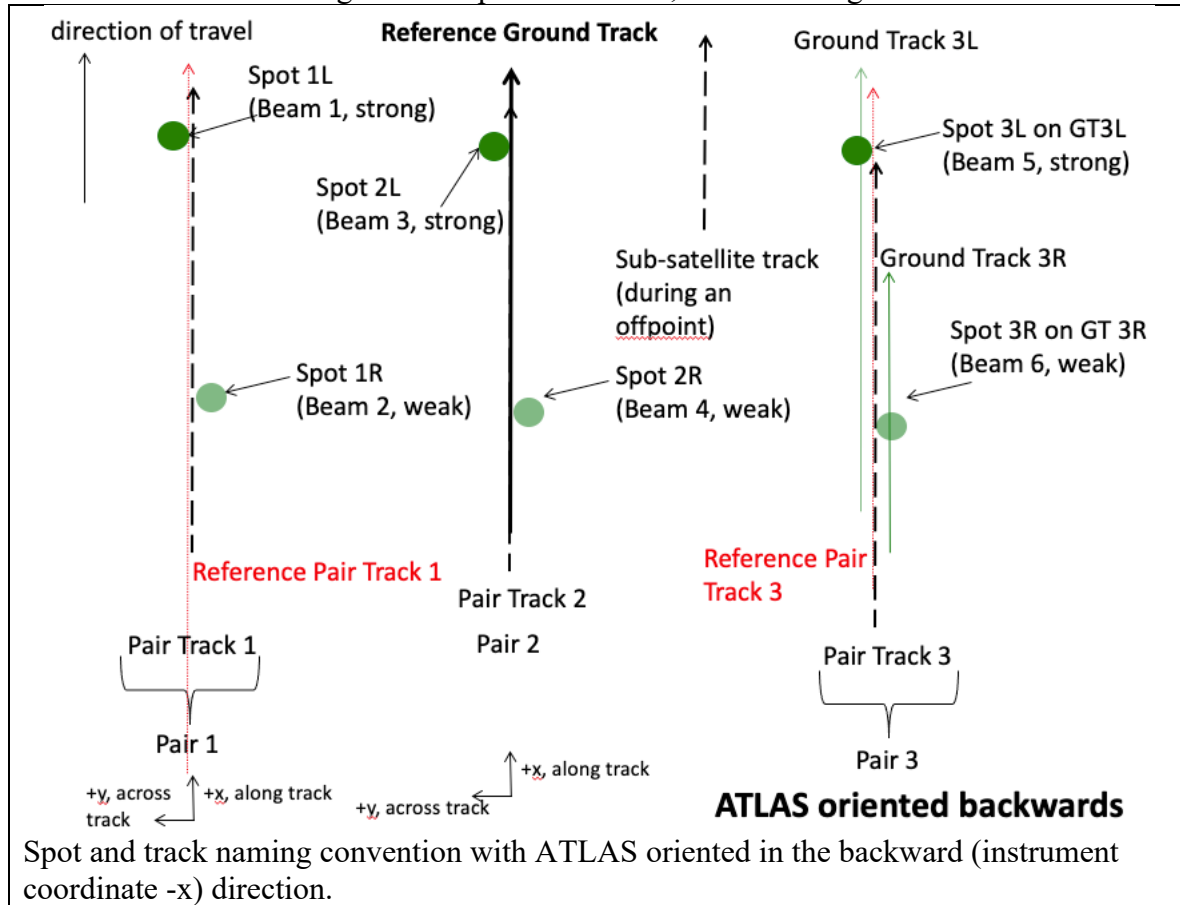
Figure 6-1. Spots and tracks, forward flight



1384
 1385

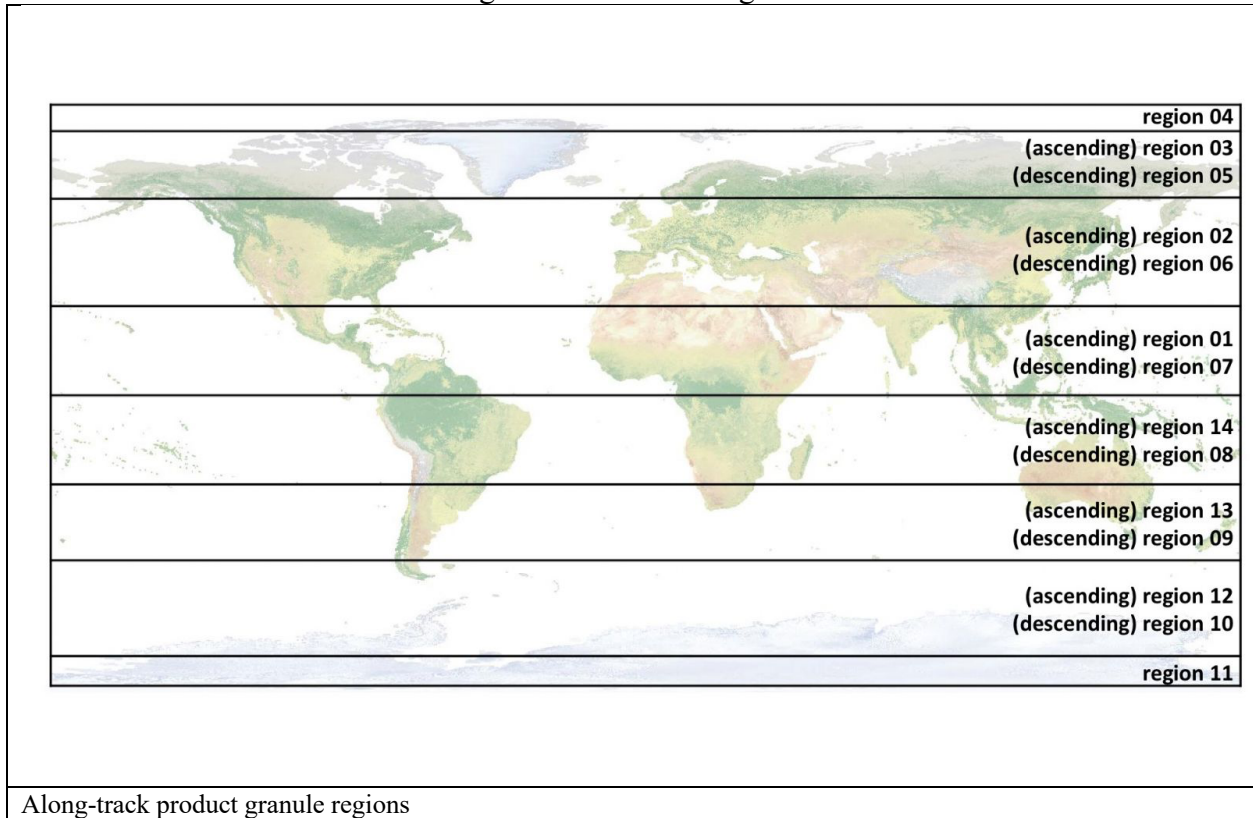
1386
 1387
 1388
 1389
 1390
 1391
 1392
 1393

Figure 6-2. Spots and tracks, backward flight



1394
 1395

Figure 6-3. Granule regions



1396 **7.0 BROWSE PRODUCTS**

1397 For each ATL11 data file, there will be eight figures written to an associated browse file. Two of
 1398 these figures are required and are located in the default group; default1 and default2. The browse
 1399 filename has the same pattern as the data filename, namely,
 1400 ATL11_tttss_c1c2_rr_vVVV_BRW.h5, where tttt is the reference ground track, ss is the orbital
 1401 segment, c1 is the first cycle of data in the file, c2 is the last cycle of data in the file, rr is the
 1402 release and VVV is the version. Optionally, the figures can also be written to a pdf file.

1403
 1404 Below is a discussion of the how the figures are made, with examples from the data file
 1405 ATL11_009403_0307_02_vU07.h5. Note that the figure numbering in this section is distinct
 1406 from that in the rest of the document; the figures shown here are labeled as they are in each
 1407 browse-product file.

1408
 1409
 1410

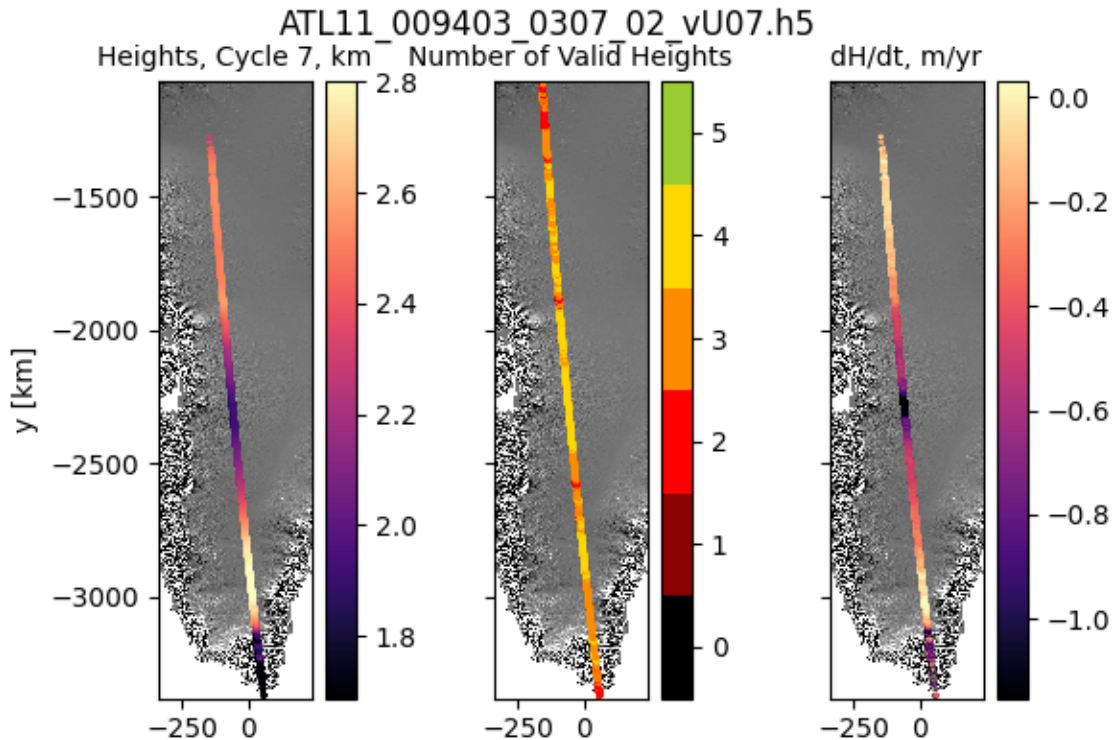


Figure 1. Height data, in km, from cycle 7 (1st panel). Number of cycles with valid height data (2nd panel). Change in height over time, in meters/year, cycle 7 from cycle 3 (3rd panel). All overlaid on gradient of DEM. x, y in km. Maps are plotted in a polar-stereographic projection with a central longitude of 45W and a standard latitude of 70N.

1411
 1412

1413 The background for the three panels in Figure 1 is the gradient DEM in gray scale. It is shown in
 1414 a polar-stereographic projection with a central longitude of 45W (0E) and a standard latitude of
 1415 70N (71S), for the Northern (Southern) Hemisphere. The map is bounded by the extent of height

1416 data plus a buffer. ATL11 heights (/ptx/h_corr) from all pairs of the latest cycle with valid data,
 1417 here cycle 7, are plotted in the first panel. The “magma” color map indicates the heights in km.
 1418 The limits on the color bar are set with the python scipy.stat.scoreatpercentile method at 5% and
 1419 95%. In the second panel are plotted the number of valid heights summed over all cycles at each
 1420 location. The color bar extends to the total number of cycles in the data file. The change in height
 1421 over time, dH/dt, is plotted in the third panel, in meters/year. dHdt is the change in height of the
 1422 last cycle with valid data from the first cycle with valid data (/ptx/h_corr) divided by the
 1423 associated times (/ptx/delta_time). Text of ‘No Data’ is printed in the panel if there is only one
 1424 cycle with valid data, or if the first and last cycles with valid data have no common reference
 1425 point numbers (/ptx/ref_pt). All plots are in x,y coordinates, in km. This figure is called
 1426 default/default1 in the BRW.h5 file.
 1427

ATL11_009403_0307_02_vU07.h5

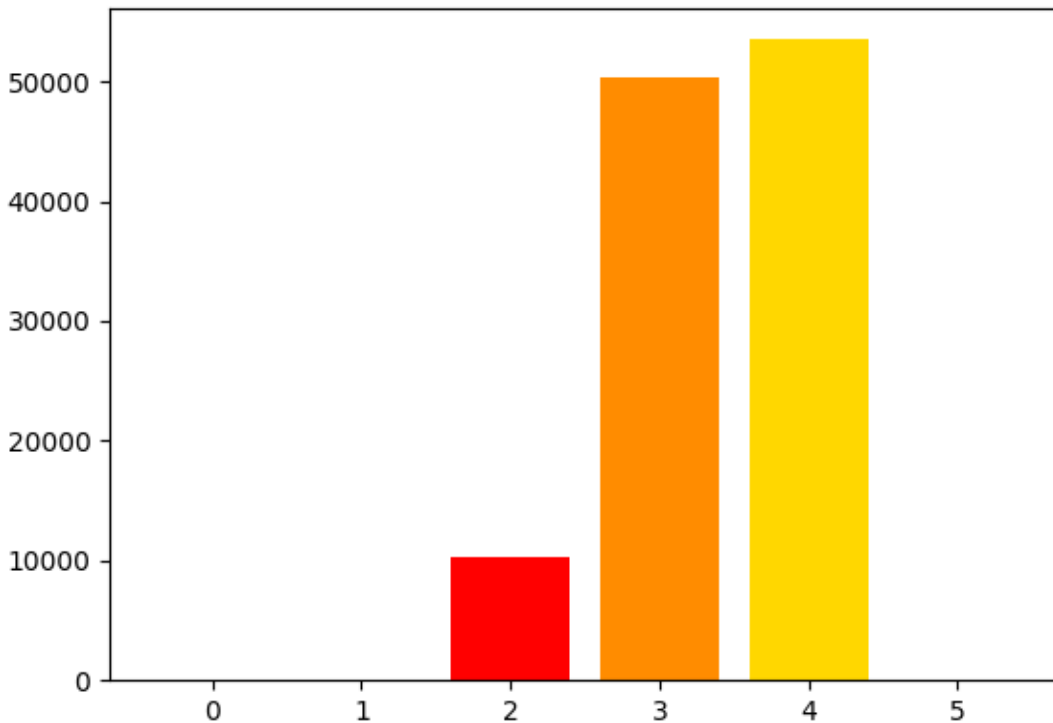


Figure 2. Histogram of number of cycles with valid height measurements, all beam pairs.

1428
 1429
 1430
 1431
 1432
 1433
 1434

A histogram of the number of valid height measurements (/ptx/h_corr) is in Figure 2. Valid height data are summed across all cycles, for each reference point number (/ptx/ref_pt). The color scale is from zero to the total number of cycles in the data file and matches those in Figure 1, 2nd panel. This figure is called validepeats_hist in the BRW.h5 file.

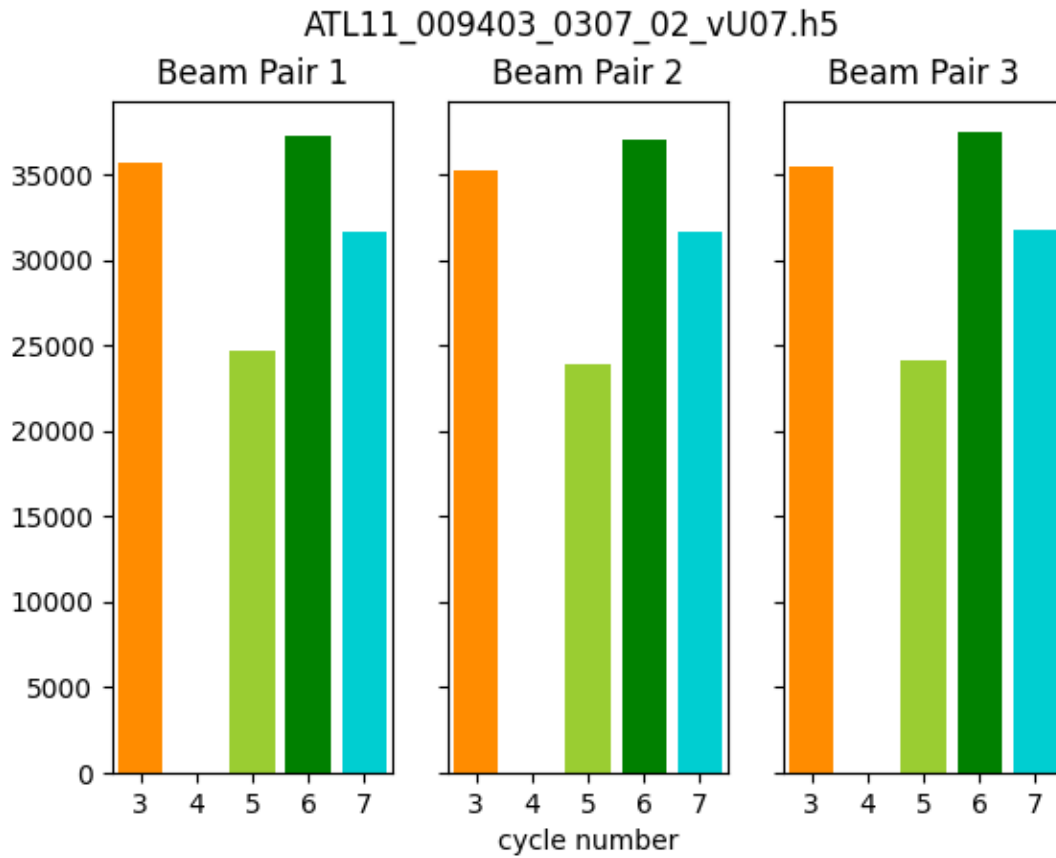


Figure 3. Number of valid height measurements from each beam pair.

1435
 1436
 1437
 1438
 1439
 1440

Histograms in Figure 3 show the number of valid heights (/ptx/h_corr) for each cycle, separated by beam pair. The cycle numbers are color coded. This figure is called default/default2 in the BRW.h5 file.

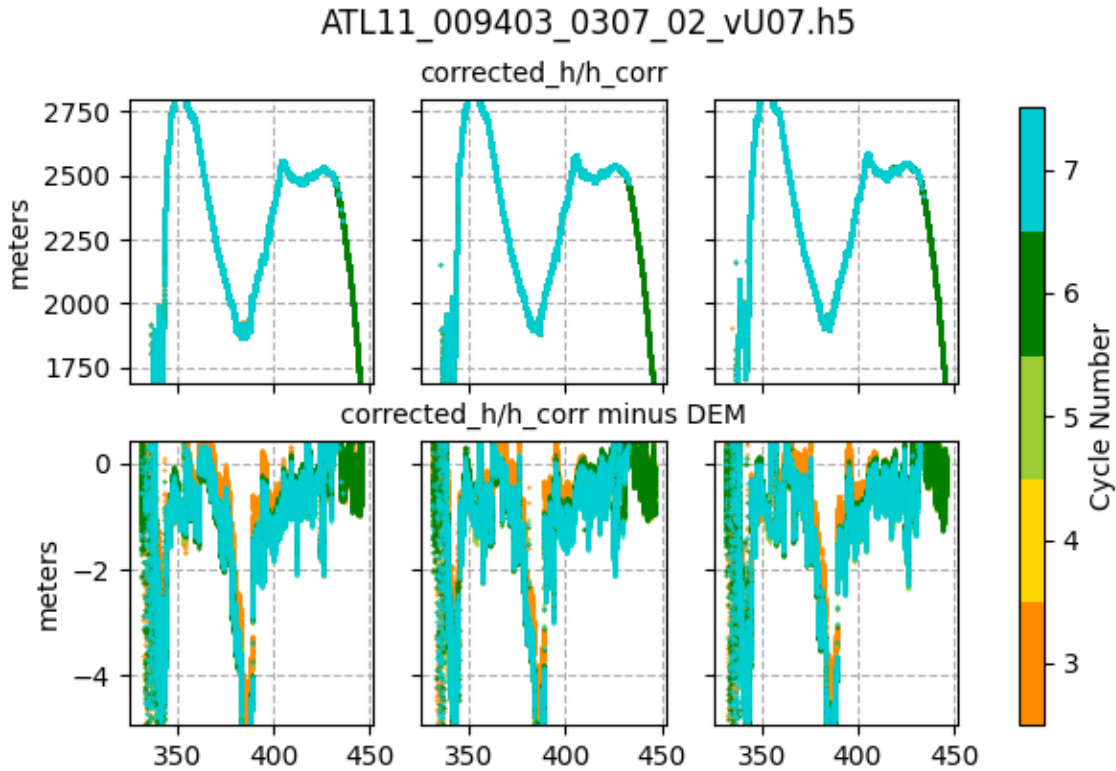


Figure 4. Top row: Heights, in meters, plotted for each beam pair: 1 (left), 2 (center), 3 (right). Bottom row: Heights minus DEM, in meters. Y-axis limits are scores at 5% and 95%. Color coded by cycle number. Plotted against reference point number/1000.

1441
 1442
 1443
 1444
 1445
 1446
 1447
 1448
 1449
 1450
 1451
 1452

There are six panels in Figure 4, with two rows and three columns. In the top row are plotted the height measurements ($/ptx/h_corr$) for each beam pair, one pair per panel. In the bottom row are plotted the same height measurements minus the collocated DEM (ref_surf/dem_h) values, one pair per panel. The plots are color coded by cycle number, as in Figure 3. The heights are plotted versus reference point number ($/ptx/ref_pt$) divided by 1000 for a cleaner plot. The y-axis is in meters for both rows. The y-axis limits for the top and bottom rows are set separately, using the python `scipy.stats.scoreatpercentile` method with limits of 5% and 95% for heights and height differences, respectively. Text of 'No Data' is printed in a panel if there are no valid height data for that pair. This figure is called `h_corr_h_corr-DEM` in the `BRW.h5` file.

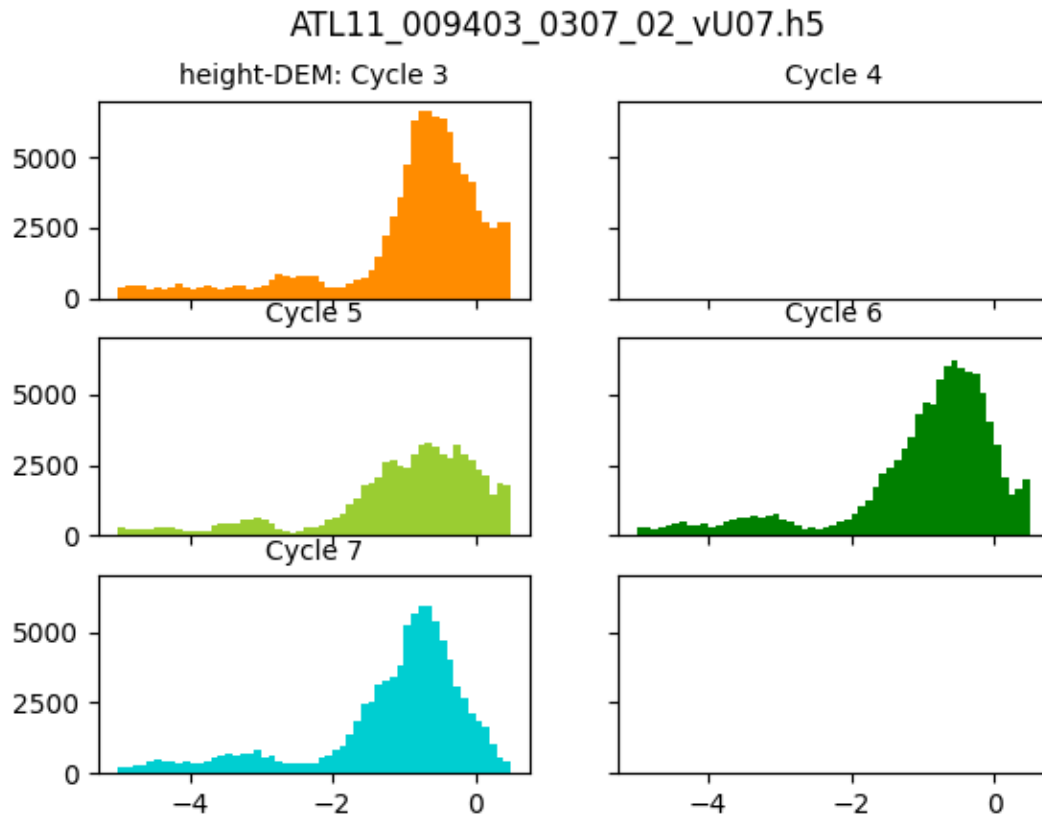


Figure 5. Histograms of heights minus DEM heights, in meters. One histogram per cycle, all beam pairs. X-axis limits are the scores at 5% and 95%.

1453
 1454
 1455
 1456
 1457
 1458
 1459
 1460
 1461

Figure 5 is associated with Figure 4. It is a multi-paneled figure, with the number of panels dependent on the number of cycles in the data file. Each panel is a histogram of the heights (/ptx/h_corr) minus collocated DEM heights (ref_surf/dem_h) color coded by cycle, the same as in Figures 3 and 4. The limits on the histograms are set using the python `scipy.stats.scoreatpercentile` method with limits of 5 and 95% for all cycles of data, the same values used in Figure 4 bottom row. This figure is called `h_corr-DEM_hist` in the BRW.h5 file.

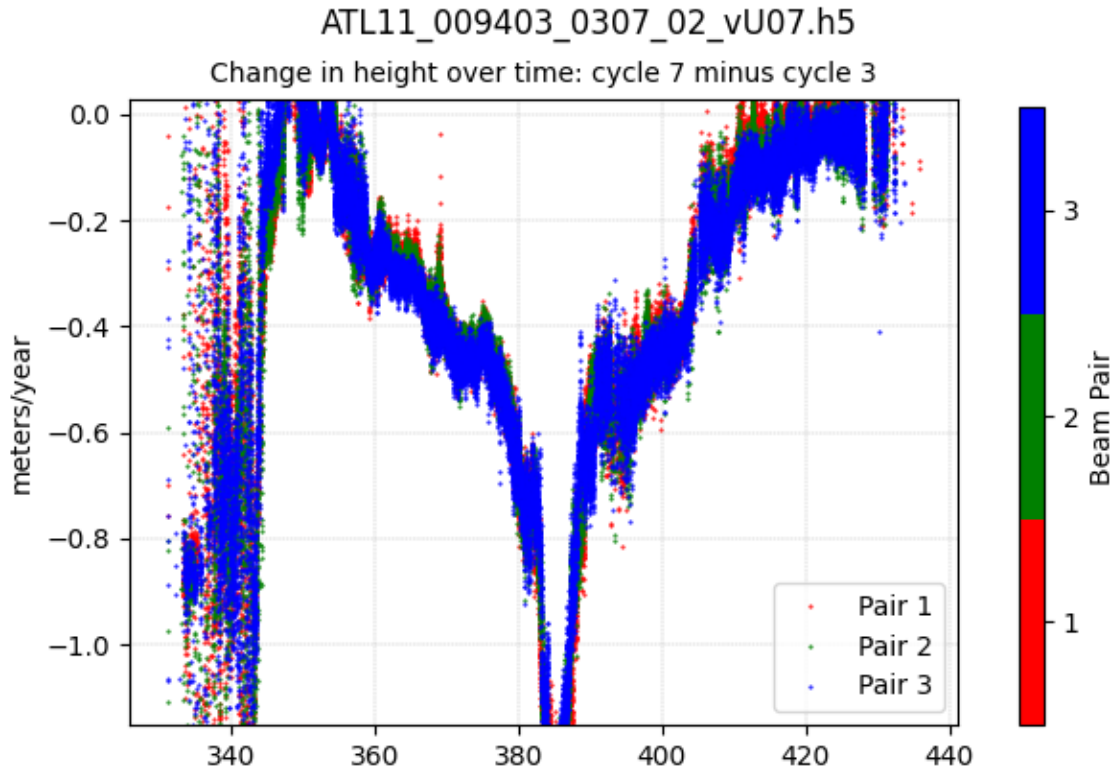


Figure 6. Change in height over time, dH/dt , in meters/year. dH/dt is cycle 7 from cycle 3. Color coded by beam pair: 1 (red), 2 (green), 3 (blue). Y-axis limits are scores at 5% and 95%. Plotted against reference point number/1000.

1462
 1463
 1464
 1465
 1466
 1467
 1468
 1469
 1470
 1471
 1472
 1473

The changes in height with time, dH/dt , in meters/year are plotted in Figure 6. The calculation differences the first and last cycles with valid height data ($/ptx/h_corr$) divided by the associated time differences ($/ptx/delta_time$). The change in heights for pair 1 are in red, for pair 2 are in green and for pair 3 are in blue. The y-axis limits are set using the python `scipy.stats.scoreatpercentile` method with limits of 5% and 95%. The x-axis is reference point number ($/ptx/ref_pt$) divided by 1000 for a cleaner plot. Text of ‘No Data’ is printed in the panel if there is only one cycle with valid data, or if the first and last cycles with valid data have no common reference point numbers. This figure is called `dHdt` in the `BRW.h5` file.

1474

Glossary/Acronyms

ASAS	ATLAS Science Algorithm Software
ATBD	Algorithm Theoretical Basis Document
ATLAS	ATLAS Advance Topographic Laser Altimeter System
CDF	Cumulative Distribution Function
DEM	Digital Elevation Model
GSFC	Goddard Space Flight Center
GTs	Ground Tracks
ICESat-2	Ice, Cloud, and Land Elevation Satellite-2
IKR	I Know, Right?
MABEL	Multiple altimeter Beam Experimental Lidar
MIS	Management Information System
NASA	National Aeronautics and Space Administration
PE	Photon Event
POD	Precision Orbit Determination
PPD	Precision Pointing Determination
PRD	Precise Range Determination
PSO	ICESat-2 Project Science Office
PTs	Pair Tracks
RDE	Robust Dispersion Estimate
RGT	Reference Ground Track
RMS	Root Mean Square
RPTs	Reference Pair Tracks
RT	Real Time
SCoRe	Signature Controlled Request
SIPS	ICESat-2 Science Investigator-led Processing System
TLDR	Too Long, Didn't Read
TBD	To Be Determined

1475

References

1476 Brunt, K.M., H.A. Fricker and L. Padman 2011. Analysis of ice plains of the Filchner-Ronne Ice
1477 Shelf, Antarctica, using ICESat laser altimetry. *Journal of Glaciology*, **57**(205): 965-975.

1478 Fricker, H.A., T. Scambos, R. Bindschadler and L. Padman 2007. An active subglacial water
1479 system in West Antarctica mapped from space. *Science*, **315**(5818): 1544-1548.

1480 Schenk, T. and B. Csatho 2012. A New Methodology for Detecting Ice Sheet Surface Elevation
1481 Changes From Laser Altimetry Data. *Ieee Transactions on Geoscience and Remote Sensing*,
1482 **50**(9): 3302-3316.

1483 Smith, B., H.A. Fricker, N. Holschuh, A.S. Gardner, S. Adusumilli, K.M. Brunt, B. Csatho, K.
1484 Harbeck, A. Huth, T. Neumann, J. Nilsson and M.R. Siegfried 2019a. Land ice height-retrieval
1485 algorithm for NASA's ICESat-2 photon-counting laser altimeter. *Remote Sensing of*
1486 *Environment*: 111352.

1487 Smith, B.E., H.A. Fricker, I.R. Joughin and S. Tulaczyk 2009. An inventory of active subglacial
1488 lakes in Antarctica detected by ICESat (2003-2008). *Journal of Glaciology*, **55**(192): 573-595.

1489 Smith, B.E., D. Hancock, K. Harbeck, L. Roberts, T. Neumann, K. Brunt, H. Fricker, A.
1490 Gardner, M. Siegfried, S. Adusumilli, B. Csatho, N. Holschuh, J. Nilsson and F. Paolo 2019b.
1491 Algorithm Theoretical Basis Document for Land-Ice Along-track Product (ATL06). Goddard
1492 Space Flight Center.

1493